NASA TECHNICAL NOTE

NASA TN D-8275 c.l
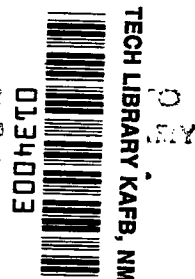
A PARAMETRIC ANALYSIS
OF VISUAL APPROACHES
FOR HELICOPTERS

Gene C. Moen, Daniel J. DiCarlo,
and Kenneth R. Yenni

Langley Research Center
Hampton, Va. 23665

NATIONAL AERONAUTICS AND SPACE ADMINISTRATION • WASHINGTON, D. C. • DECEMBER 1976

1. Report No. NASA TN D-8275	2. Government Accession No.	3. Recipient's Catalog No.
4. Title and Subtitle A PARAMETRIC ANALYSIS OF VISUAL APPROACHES FOR HELICOPTERS		5. Report Date December 1976
		6. Performing Organization Code
7. Author(s) Gene C. Moen, Daniel J. DiCarlo, and Kenneth R. Yenni		8. Performing Organization Report No. L-10841
9. Performing Organization Name and Address NASA Langley Research Center and Langley Directorate, USAAMRDL Hampton, VA 23665		10. Work Unit No. 505-10-23-01
		11. Contract or Grant No.
12. Sponsoring Agency Name and Address National Aeronautics and Space Administration Washington, DC 20546 and U.S. Army Air Mobility R&D Laboratory Moffett Field, CA 94035		13. Type of Report and Period Covered Technical Note
		14. Army Project No. IF262209AH76

15. Supplementary Notes

Gene C. Moen: Langley Directorate, U.S. Army Air Mobility R&D Laboratory.

Daniel J. DiCarlo and Kenneth R. Yenni: Langley Research Center.

16. Abstract

     A flight investigation was conducted to determine the characteristic shapes of the altitude, ground-speed, and deceleration profiles of visual approaches for helicopters. Two hundred and thirty-six visual approaches were flown from nine sets of initial conditions with four types of helicopters. Mathematical relationships were developed that describe the characteristic visual deceleration profiles. These mathematical relationships were expanded to develop equations which define the corresponding nominal ground-speed, pitch-attitude, pitch-rate, and pitch-acceleration profiles. Results are applicable to improved helicopter handling qualities in terminal-area operations.

17. Key Words (Suggested by Author(s)) Helicopter and VTOL approaches Visual approach Approach profiles Instrument approach Terminal-area operations	18. Distribution Statement Unclassified — Unlimited Subject Category 08

19. Security Classif. (of this report) Unclassified	20. Security Classif. (of this page) Unclassified	21. No. of Pages 39	22. Price* $3.75

A PARAMETRIC ANALYSIS OF VISUAL APPROACHES FOR HELICOPTERS

Gene C. Moen,* Daniel J. DiCarlo, and Kenneth R. Yenni
Langley Research Center

SUMMARY

A flight investigation was conducted to determine the characteristic shapes of the altitude, ground-speed, and deceleration profiles of visual approaches for helicopters. Two hundred and thirty-six visual approaches were flown from nine sets of initial conditions with four types of helicopters. Mathematical relationships were developed that describe the characteristic visual deceleration profiles. These mathematical relationships were expanded to develop equations which define the corresponding nominal ground-speed, pitch-attitude, pitch-rate, and pitch-acceleration profiles.

INTRODUCTION

Numerous studies have been undertaken to improve the instrument flight capability of helicopters during the final approach phase of flight. Various instrument approach procedures have been studied ranging from the standard straight-in ILS (instrument landing system) approach to the more complicated curved, decelerating, variable-glide-slope approach. A typical method of attack during these investigations has been to predefine a set of approach parameters (for example, altitude and velocity profile shapes) and investigate them under simulated instrument flight conditions. In many instances, even though the predefined parameters were valid to accomplish the task safely, pilots were reluctant to follow the guidance precisely to accomplish the desired profile because of "unnatural" physiological cues. A typical comment was, "It feels like the helicopter is 'falling out' during flare." It was believed that "natural" cues were those physiological cues associated with approaches conducted under visual flight conditions. It followed that an analysis of typical VFR (Visual Flight Rules) approaches might identify what constitutes a "natural feeling" approach. This information could then be incorporated into the IFR (Instrument Flight Rules) schemes under investigation.

The present investigation was undertaken to measure and define the characteristic shapes of various visual approach profiles. The approach parameters of ground speed and altitude were measured and recorded as functions of range, and the data were

---

*Langley Directorate, U.S. Army Air Mobility R&D Laboratory.

subsequently processed to determine the average (nominal) profiles for ground speed, altitude, and deceleration. In addition, parametric and graphical analysis techniques were used to develop a mathematical representation of the deceleration profiles, and these results were further used to develop analytical expressions for defining ground-speed, pitch-attitude, pitch-rate, and pitch-acceleration profiles.

The results from this study have several potential uses. First, knowledge of how pilots fly visual approaches will be of value in assessing pilot comments from instrument approach studies. Also, continuous mathematical functions have been developed which describe the characteristic visual deceleration and ground-speed profiles; these equations could be used to develop instrument approach control laws and to define further the corresponding hardware requirements. In addition, knowledge of the visual-profile characteristics should be of value to traffic control planners in developing or assessing terminal-area traffic control procedures.

SYMBOLS

The units for physical quantities defined in this paper are given in both the International System of Units (SI) and U.S. Customary Units. All measurements and calculations were made in U.S. Customary Units. Factors relating the two systems are given in reference 1. Secondary scales, incorporating U.S. Customary Units, are included in several figures to assist the user in developing instrument approach profiles compatible with existing aircraft instrumentation.

c	constant (see eq. (3))
g	acceleration due to gravity ($1g = 9.8$ m/sec^2 (32.2 ft/sec^2))
k	constant, $\frac{1}{c}$ (see eq. (4))
m	slope of the ground-speed profile curve, sec^{-1}
n	exponential term
q	pitch rate, deg/sec
$\dot{q}$	pitch acceleration, deg/sec^2
t	time, sec

2

| x,y,z | coordinates in rectangular coordinate system, m (ft) (see fig. 3) |

$\dfrac{\partial F_X}{\partial u}$ longitudinal drag coefficient, $\sec^{-1}$ (see eq. (8))

γ flight-path angle, deg

θ pitch attitude of the aircraft relative to the pitch attitude for hover (pitch-up positive), deg

Subscripts:

d   initial condition for a variable at the start of the deceleration maneuver (Range = 850 m (2800 ft))

max   maximum

A dot over a symbol indicates the first derivative with respect to time; two dots indicate the second derivative.

DESCRIPTION OF TESTS

Test Vehicles and Facilities

Four types of helicopters, shown in figure 1, were used in the present investigation; they were selected to represent a cross section of operational helicopters. The general characteristics of each helicopter are shown in table I. Each cockpit was equipped with the standard instruments for that aircraft.

All tests were conducted at the NASA Wallops Flight Center and used a GSN-5 precision tracking radar (fig. 2) to determine and record the helicopter positions and velocities in a rectangular coordinate system (fig. 3), the origin of which was located at the center of the landing pad. A description of the radar is contained in the appendix. During each approach, altitude, cross range, and ground speed were recorded as functions of range on x-y plotters. These plots were subsequently processed to determine the characteristic profile shapes for visual approaches.

Task Description

The pilots' task was to fly a descending, decelerating, visual approach having a predetermined set of initial conditions and terminating in a 12-m (40-ft) hover over a landing pad. All approaches were started at a range in excess of 3 km (10 000 ft) and

3

one of nine sets of initial airspeed and altitude conditions (fig. 4) was used. The pilots were instructed to fly what they considered to be a visual approach from the given set of initial conditions and to assume that there were commercial passengers aboard the aircraft. In addition, they were instructed to avoid abrupt maneuvers and to maintain the given initial altitude and airspeed conditions until they initiated either the descent or deceleration portion of the approach. No approach guidance was provided except for the standard aircraft instruments normally used for visual approaches. The task was complete when the aircraft was brought to a hover over the landing pad.

FLIGHT RESULTS

Two hundred and thirty-six approaches were flown by both NASA research pilots and military test pilots. All test subjects were proficient and experienced in the helicopter types used in the present investigation. During each approach, the variables of altitude and ground speed were recorded as functions of range. These plots were then processed to determine the arithmetic average values and standard deviations at selected range intervals. For the purpose of this study, the resulting plots of the arithmetic average as a function of range were used to provide the characteristic shape for the visual profiles, and the standard-deviation envelopes provided an indication of how the individual profiles varied with respect to the characteristic shape. Initially, the data were analyzed in terms of the individual helicopter types, and the differences caused by these variations were determined to be minimal.

Altitude Profiles

The altitude profile results are shown in figures 5 to 7. Shown in figure 5 are six individual altitude profiles which were obtained during the tests and are presented here as being representative of the multitude of flight data obtained. The approaches from which these data were taken were initiated at an altitude of approximately 300 m (1000 ft) and from three different airspeed initial conditions. Also, these data represent the results from only one test subject in only one helicopter type.

The arithmetically averaged profiles for each of the nine sets of initial conditions are shown in figure 6. A review of these profiles indicates that the pilots fly a concave-down flight path until they obtain an average value ranging from 6.5° to 12.5°. Following the concave-down segment, the pilots fly a straight-line segment, terminating with a concave-up segment which starts approximately 300 m (1000 ft) from the hover point. A further review of these results indicates that a decrease in the initial airspeed results in an increased nominal flight-path angle; conversely, a decrease in the initial altitude results in a decreased nominal flight path.

4

The altitude standard-deviation envelopes are shown in figure 7. A review of this figure indicates that the standard deviation, which is a measure of profile repeatability, varied primarily as a function of the altitude initial condition and was not significantly affected by variations in the airspeed initial condition.

Ground-Speed Profiles

The results for the ground-speed profiles are shown in figures 8 to 10. Shown in figure 8 are five typical ground-speed profiles which again represent actual flight-test data obtained from a single test subject and a single helicopter type. The visual approaches from which these data were taken were initiated from an 80-knot airspeed initial condition and from three different altitude initial conditions, as shown in the figure.

The arithmetically averaged ground-speed profiles (fig. 9) have been grouped by their airspeed initial conditions, and all profiles exhibit the same characteristic shape. A review of these nominal profiles indicates that there is a tendency to fly a slightly faster approach when the approach is initiated from the lower altitudes. The ground-speed standard-deviation envelopes are shown in figure 10. A review of this figure indicates that the ground-speed standard-deviation values were significantly larger for the 100-knot (high-speed) approaches than for either the 80- or 50-knot approach. From discussions with one of the test subjects, it is believed that the larger standard-deviation envelopes were caused by the pilot task requirement for holding the initial airspeed until he initiated the deceleration maneuver. Furthermore, this test subject indicated that, in the absence of the defined task, he would have preferred to have slowed the approach speed to approximately 80 knots at a range of approximately 2 n. mi. which, in turn, would probably have resulted in ground-speed profiles similar to the 80-knot profiles shown in figure 10.

Visual Deceleration Profiles

The visual deceleration profiles are shown in figure 11. These profiles specifically represent the component of deceleration measured along the X-axis of the coordinate system. The circles shown in the figure represent the average deceleration value at that specific range and were obtained by graphically differentiating the arithmetic average ground-speed profiles shown in figure 10. The equation which was used to compute the deceleration levels at the various range points was derived from the equation for the slope of the ground-speed profile, which is

$$m = \frac{d\dot{x}}{dx} \qquad (1)$$

Dividing both sides of equation (1) by dt and rearranging yield

$$\ddot{x} = m\dot{x} \tag{2}$$

where m is the slope of the ground-speed profile and $\dot{x}$ is the ground-speed value at the specific range points.

Graphical differentiation methods usually result in a scatter of the differentiated values, and this feature was observed in the slight scatter of the circles shown in figure 11. However, even with the slight scatter, the circles reasonably define the characteristic shape of the nominal deceleration profiles. These visual deceleration profiles exhibit a concave-up characteristic over a major portion of the deceleration maneuver, which builds up to a maximum level at approximately 60 m (200 ft) from the landing pad. For eight of the nine initial-condition cases investigated, the maximum nominal values of deceleration varied between 0.14g and 0.19g. The remaining case was the low-altitude, high-speed approach which had a maximum nominal deceleration level of 0.24g.

ANALYTICAL RESULTS

The flight-test results were analyzed further by using parametric and graphical techniques, and the analysis has led to the development of mathematical relationships that describe the nominal deceleration, ground-speed, pitch-attitude, pitch-rate, and pitch-acceleration profiles for visual approaches. The best parametric results were obtained when the parameter $\dfrac{\dot{x}^2}{\ddot{x}}$ was plotted as a function of x on log-log paper. One example of this parametric plot is shown in figure 12. The data points represent computed values of the parameter $\dfrac{\dot{x}^2}{\ddot{x}}$ for the 100-knot, 300-m (1000-ft) case, and the ground-speed and deceleration values used to compute these points were taken from figures 10(h) and 11(h), respectively, before the figures were reduced for this report.

The form of the equation for a straight-line plot on log-log paper is given in reference 2 and, for the parametric plot shown in figure 12, yields the following equation:

$$\frac{\dot{x}^2}{\ddot{x}} = cx^n \tag{3}$$

where n is the geometric slope of the straight line and c is the ordinate intercept for $x = 1$.

Algebraic rearrangement and substitution yield the following equation for deceleration:

$$\ddot{x} = \frac{k\dot{x}^2}{x^n} \tag{4}$$

6

where $\ddot{x}$ is in m/sec^2 (ft/sec^2) and k is equal to the reciprocal of c. (This reciprocal relationship is used in the development of all following equations.)

Nominal Deceleration Profiles

Analysis of the flight-test data has indicated that the nominal deceleration profiles have the form of equation (4). The accuracy of this representation was evaluated by comparing the actual flight-test data with deceleration profiles obtained from equation (4) using suitable values for n and k.

Values for n were obtained by plotting the parameter $\dfrac{\ddot{x}^2}{\dddot{x}}$ against range x for each of the nine flight-test cases and then measuring the geometric slope of the straight-line approximation which was drawn through the data points. (An example of these plots was previously discussed and is shown in fig. 12.) The constant k can be evaluated by substituting known values of ground speed and deceleration at any initial range x_d into equation (4) and solving for k as follows:

$$k = \frac{x_d^{\,n}}{\dot{x}_d^{\,2}} \ddot{x}_d \tag{5}$$

The range x_d for starting the deceleration maneuver computations was selected at 850 m (2800 ft) because, for all approaches, 80 percent or more of the deceleration took place within the last 850 m (2800 ft) of range. The corresponding initial ground speed $\dot{x}_d$ was obtained from the arithmetic average ground-speed profiles (fig. 10).

The initial deceleration level $\ddot{x}_d$ was first estimated from the flight deceleration data (fig. 11), and then, through an iterative process, subsequent values were selected for $\ddot{x}_d$ until the continuous curves fit the flight deceleration data points reasonably well. These analytically derived profiles were then superimposed on the flight deceleration data as shown in figure 13. It can be seen that equation (4) provides a close mathematical description of the flight-test data for each of the nine sets of initial conditions.

After determining the values of n and $\ddot{x}_d$ (which is used to compute k) for each of the cases, it was recognized that a relationship existed between these values and the initial ground speed $\dot{x}_d$. Shown in figure 14 is a plot of the exponential term n as a function of initial ground speed $\dot{x}_d$. It can be seen that the values of n tend to decrease as values of $\dot{x}_d$ increase. Furthermore, a smooth curve (as indicated by the dashed line) can be passed through seven of the nine data points, which, in turn, implies an empirical relationship between these two parameters. After obtaining the final values for $\ddot{x}_d$, it was again noted that these values varied basically as a function of $\dot{x}_d$; this relationship has been plotted in figure 15. Again, seven of the nine data points can be connected by a smooth curve. The significance of the dashed curves shown in figures 14 and 15 is that

7

these curves relate the exponential term n and the constant k to the common parameter $\dot{x}_d$.

Nominal Ground-Speed Profiles

By inspection, it can be seen that the $\dfrac{k\dot{x}}{x^n}$ portion of the second term of equation (4) is equal to the factor m in equation (2), which, in turn, is defined as $\dfrac{d\dot{x}}{dx}$ in equation (1). This inspection and subsequent substitution leads to the following differential equation:

$$\frac{d\dot{x}}{\dot{x}} = \frac{k\,dx}{x^n} \tag{6}$$

Integrating equation (6) between corresponding limits yields

$$\int_{\dot{x}_d}^{\dot{x}} \frac{d\dot{x}}{\dot{x}} = \int_{x_d}^{x} \frac{k\,dx}{x^n}$$

or

$$\ln\frac{\dot{x}}{\dot{x}_d} = \frac{kx^{1-n}}{1-n} - \frac{kx_d^{1-n}}{1-n}$$

and solving for $\dot{x}$ yields

$$\dot{x} = \dot{x}_d e^{\frac{-k}{1-n}\left(x^{1-n} - x_d^{1-n}\right)} \tag{7}$$

where $\dot{x}$ is in m/sec (ft/sec).

The ground-speed profiles shown in figure 16 were computer-generated by using equation (7). Direct comparison of these profiles with the average ground-speed profiles obtained from flight data (fig. 10) indicates that equation (7) provides an extremely close reproduction of the flight-test data.

Nominal Pitch-Attitude Profiles

An approximate value for the nominal pitch attitude can be determined from the following equation:

$$\theta \approx \frac{57.3}{g}\left[\ddot{x} + \left(\frac{\partial F_X}{\partial u}\right)\dot{x}\right] \tag{8}$$

where $\dfrac{\partial F_X}{\partial u}$ corresponds to the stability derivative X_u in the body force equations on page 124 of reference 3.

Substituting equation (4) into equation (8) yields the following equation for the nominal pitch-attitude profiles:

$$\theta \approx \frac{57.3}{g}\left[\frac{k\dot{x}^2}{x^n} + \left(\frac{\partial F_X}{\partial u}\right)\dot{x}\right]$$ (9)

where θ is in degrees and is measured with respect to the hover pitch attitude (pitch-up positive).

Nominal pitch-attitude profiles were obtained from computer solutions of equation (9). In these solutions, a value of 0.025 sec^{-1} was used for the longitudinal drag coefficient $\frac{\partial F_X}{\partial u}$ and was based on flight-test data from helicopter 3. It should be noted that $\frac{\partial F_X}{\partial u}$ varies depending upon the aircraft; for example, flight-test results from helicopter 4 yield a value of 0.019 sec^{-1} for $\frac{\partial F_X}{\partial u}$. Thus, when applying equation (9) to a specific aircraft, an appropriate value should be used for the coefficient.

The nominal pitch-attitude profiles (fig. 17) exhibit the same characteristic shape as the nominal deceleration profiles (fig. 13). Furthermore, the maximum pitch values occur at approximately the same range (x = 60 m (200 ft) from the landing pad) as the maximum deceleration values. In all cases but one, the maximum nominal pitch values varied from 7° to 8.5^O. The one exception was the low-altitude, high-speed approach (fig. 17(g)) which had a maximum value approaching 11.5^O. This exception is consistent with the deceleration profile results (fig. 13(g)), wherein the same case resulted in the highest maximum deceleration value.

Nominal Pitch-Rate Profiles

An equation for pitch rate can be obtained by differentiating equation (9) with respect to time and by further substituting equation (4) into the differentiated expression. This yields

$$q \approx \frac{57.3k}{g}\left[\frac{2k\dot{x}^3}{x^{2n}} - \frac{n\dot{x}^3}{x^{n+1}} + \left(\frac{\partial F_X}{\partial u}\right)\frac{\dot{x}^2}{x^n}\right]$$ (10)

where q is in deg/sec.

The nominal pitch-rate profiles which were obtained by using equation (10) are shown in figure 18. A review of this figure indicates that the nominal pitch-rate values gently increase up to a point approximately 120 m (400 ft) from the landing pad. A further review of the figure indicates that the highest nominal pitch rates are negative (pitch-down), approach or exceed -1.0 deg/sec, and occur at a range of approximately 12 m (40 ft) from the landing pad.

Nominal Pitch-Acceleration Profiles

The pitch-acceleration equation can be derived by differentiating equation (10) with respect to time and by further substituting equation (4) into the differentiated expression. This yields the following equation:

$$\dot{q} \approx \frac{57.3}{g}\left\{\left[\frac{6k^3\dot{x}^4}{x^{3n}} - \frac{7nk^2\dot{x}^4}{x^{2n+1}} + \frac{n(n+1)k\dot{x}^4}{x^{n+2}}\right] + \frac{\partial F_X}{\partial u}\left(\frac{2k^2\dot{x}^3}{x^{2n}} - \frac{nk\dot{x}^3}{x^{n+1}}\right)\right\} \tag{11}$$

The nominal pitch-acceleration profiles are shown in figure 19 and were computer-generated by using equation (11). A review of these profiles indicates that the highest pitch accelerations are also negative, vary from -0.17 to -0.62 deg/sec^2, and occur at a range of approximately 36 m (120 ft).

Visual Profile Summary

With the exception of the ground-speed profile, all profiles achieved their maximum values during the last 120 m (400 ft) of the approach. These maximum values have been tabulated in a matrix format and are shown in figure 20.

Subelement A of this matrix contains the value of the nominal time interval required to complete the last 850 m (2800 ft) of the approach. These time interval values were obtained directly from the computer listings while generating the nominal deceleration profiles shown in figure 13. A review of the matrix indicates that these time intervals varied from 41 to 94 sec and that the low-speed approaches involved the longest time intervals.

DISCUSSION

Significance of Pitch-Axis Profiles

During a helicopter decelerating approach, the pitch axis is the primary control axis because deceleration is primarily a function of pitch attitude. This is verified by the fact that most of the adverse pilot comments received during helicopter instrument approach studies have dealt with pitch-axis control inputs during the latter portion of the deceleration maneuver. For example, in reference 4 it is indicated that both the linear deceleration profiles (i.e., ground speed was a linear function of range) and the constant deceleration profiles yield undesirable pitch-axis control characteristics close to the hover point. Specifically, the linear deceleration profiles resulted in the pilot's impression that he was being commanded to hover well short of the touchdown point, and the constant deceleration profiles resulted in the pilot's objecting to a high-pitch—low-power condition when coming to a hover.

10

An analysis of the visual approach data indicates that, under visual conditions, the pitch-axis control activity increases significantly during the last 120 m (400 ft) of the approach. Furthermore, this is the same region of the approach where the helicopter is in transition to the hover condition and is also the same region wherein the unnatural physiological cues have been encountered during instrument approach studies.

Application of Mathematical Relationships

The mathematical relationships developed in this study can be used to define instrument approach profiles which potentially do not result in unnatural physiological cues that have been encountered on some of the previous instrument studies. However, before applying these relationships, it is necessary for the user to select values for the exponential term n and the coefficient k. Values for n can be selected from the curve shown in figure 21. This curve is based on the flight-test data shown in figure 14 and represents a smooth curve drawn through seven of the nine data points.

The coefficient k can be computed by using equation (5); however, before using the equation, it is necessary to select initial values for the variables on the right-hand side of the equation. A value of 850 m (2800 ft) should be used as the value for x_d because the flight-test data and the subsequent development of mathematical relationships were based on that value for the initial range. A value for the initial ground speed $\dot{x}_d$ can be selected at the discretion of the user. After selecting the initial ground speed the user must determine the initial deceleration level $\ddot{x}_d$. A value for $\ddot{x}_d$ can be selected from one of the curves shown in figure 22. During this study, it was found that the maximum (peak) deceleration could be varied by varying the initial deceleration level. Thus, a number of computer runs were made by using an iterative process to determine the initial deceleration values which produced maximum deceleration peaks ranging from 0.10g to 0.16g in 0.02g increments. The four curves (fig. 22) represent the results from the computer study and can be used to select the initial deceleration level.

In applying these results to instrument approach profiles, it would be desirable for the user to program the equations on a computer and subsequently to analyze the profiles in terms of the defined task. For example, the 0.16g deceleration profiles, in general, resulted in larger peak values for pitch attitude, pitch rate, and pitch acceleration than were shown in the corresponding profiles obtained from the nominal flight-test results. Thus, the 0.16g profiles would probably result in a high pilot workload during the last portion of the deceleration maneuver.

Summary of Computer-Generated Profiles

The data matrix (fig. 23) has been included in this report in an effort to assist future users of these data. The numerical values presented in the matrix were obtained from

computer-generated profiles that, in turn, were based on using the curves shown in figures 21 and 22 to determine the values for n and k. Each column represents different initial ground-speed conditions $\dot{x}_q$, and each row represents different maximum deceleration levels varying from 0.10g to 0.16g in 0.02g increments. As shown in the figure key, the upper left subelement is the time interval required to complete the last 850 m (2800 ft) of the approach, and the remaining subelements are the numerical peak values for pitch attitude, pitch rate, and pitch acceleration. In addition, a number of the subelements have been hatched in an effort to point out particular features of specific profiles.

Specifically, the upper left-hand subelements have been hatched where the time interval exceeded 94 sec, which was the longest corresponding time interval for the visual approach data. Thus, it is believed that a deceleration time interval that significantly exceeds 94 sec will probably result in a prolonged deceleration maneuver with corresponding adverse pilot comments.

The remaining subelements have been hatched where the peak value for that respective pitch parameter exceeded the corresponding lowest peak value obtained from the nominal flight-test results. For example, a review of figure 20 indicates that the lowest peak value for pitch attitude was 7.14^{o}. Thus, all peak pitch-attitude values that exceeded 7.14^{o} have been hatched in figure 23.

In presenting these results, it should be pointed out that the hatching was not intended to eliminate that profile from consideration, but rather to point out any potentially adverse characteristics of that profile. Similarly, several profiles shown in the matrix have no subelements which have been hatched, and these have been designated by a dark border.

CONCLUSIONS

A flight investigation has been made to determine whether a characteristic shape exists for approach profiles utilized by helicopters under visual conditions. Generally, such was found to be the case, and variations in the characteristic shapes of the profiles caused by differences in initial conditions were determined. Based on the results of this study, the following conclusions were drawn:

1. Mathematical expressions were developed that closely describe the nominal ground-speed and deceleration profiles obtained during flight tests.

2. All visual approach altitude profiles had nominal flight-path values ranging from 6.5^{o} to 12.5^{o} and exhibited a concave-up characteristic over approximately the last 300 m (1000 ft) of the approach.

3. The maximum values for the nominal deceleration levels varied between 0.14g and 0.24g and occurred at a range of approximately 60 m (200 ft) from the landing pad.

4. Under visual conditions, the pitch-axis control activity increases significantly during the last 120 m (400 ft) of the approach.

5. The maximum values for the nominal pitch attitude occurred at approximately the same range as the maximum deceleration values (60 m (200 ft) from the landing pad) and varied from approximately 7° to 11.5^O (nose-up).

6. The maximum values for the nominal pitch rates are negative, approach or exceed -1.0 deg/sec, and occur within the last 12 m (40 ft) of the approach in a region where the pilot is establishing a hover condition.

7. The highest nominal pitch acceleration levels were negative (pitch-down), varied from -0.17 to -0.62 deg/sec^2, and occurred at an approximate range of 36 m (120 ft).

APPENDIX

DESCRIPTION OF TRACKING RADAR

The GSN-5 precision tracking radar measures the position of aircraft in terms of slant range, azimuth, and elevation angles of the radar antenna. Data from this spherical coordinate system are transformed into the rectangular coordinate system shown in figure 3. Transformed aircraft data — both positions and rates — are recorded on standard x-y plotters. A passive corner reflector is mounted on the nose of the aircraft to prevent skin tracking.

The GSN-5 is a K-band radar and has an antenna beam width of approximately 0.5°. This radar is capable of tracking from 0° to 30° in elevation and from 45° to -45° in azimuth. Position uncertainties in rectangular coordinates are shown in the following table:

Range		Position uncertainty in coordinate —					
		x		y		z	
km	ft	m	ft	m	ft	m	ft
0	0	5	16.4	1	3.28	1	3.28
4	13 150	36	1·18	2.5	8.2	3.2	10.5

14

REFERENCES

1. Mechtly, E. A.: The International System of Units – Physical Constants and Conversion Factors (Second Revision). NASA SP-7012, 1973.

2. Franklin, Philip: Graphical Representation of Functions. Mark's Mechanical Engineers' Handbook, Sixth ed., Theodore Baumeister, ed., McGraw-Hill Book Co., Inc., 1958, pp. 2-79 – 2-91.

3. Etkin, Bernard: Dynamics of Flight. John Wiley & Sons, Inc., c.1959.

4. Kelly, James R.; Niessen, Frank R.; Thibodeaux, Jerry J.; Yenni, Kenneth R.; and Garren, John F., Jr.: Flight Investigation of Manual and Automatic VTOL Decelerating Instrument Approaches and Landings. NASA TN D-7524, 1974.

TABLE I.- GENERAL CHARACTERISTICS OF TEST VEHICLES

Characteristic	Helicopter 1	Helicopter 2	Helicopter 3	Helicopter 4
Type	Light observation	Light utility	Medium transport	Medium transport
Maximum gross weight	12 233 N (2750 lb)	37 810 N (8500 lb)	68 947 N (15 500 lb)	84 961 N (19 100 lb)
Maximum airspeed	115 knots	120 knots	120 knots	142 knots
Configuration	Single rotor	Single rotor	Tandem rotor	Single rotor
Disk loading	148.4 Pa (3.1 lb/ft^2)	225.0 Pa (4.7 lb/ft^2)	201.1 Pa (4.2 lb/ft^2)	301.6 Pa (6.3 lb/ft^2)
Power plant	Single turbine	Single turbine	Twin turbine	Twin turbine
Total power	410 kW (550 hp)	820 kW (1100 hp)	1565 kW (2100 hp)	1565 kW (2100 hp)
Control stabilization	None	Augmented rate (gyro bar)	Rate	Attitude

(a) Light observation; helicopter 1.

(b) Light utility; helicopter 2.
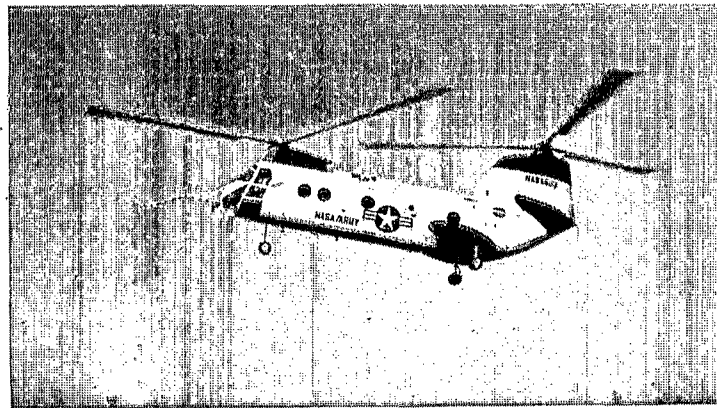
(c) Medium transport; helicopter 3.

(d) Medium transport; helicopter 4.

L-76-234

Figure 1.- Test helicopters.
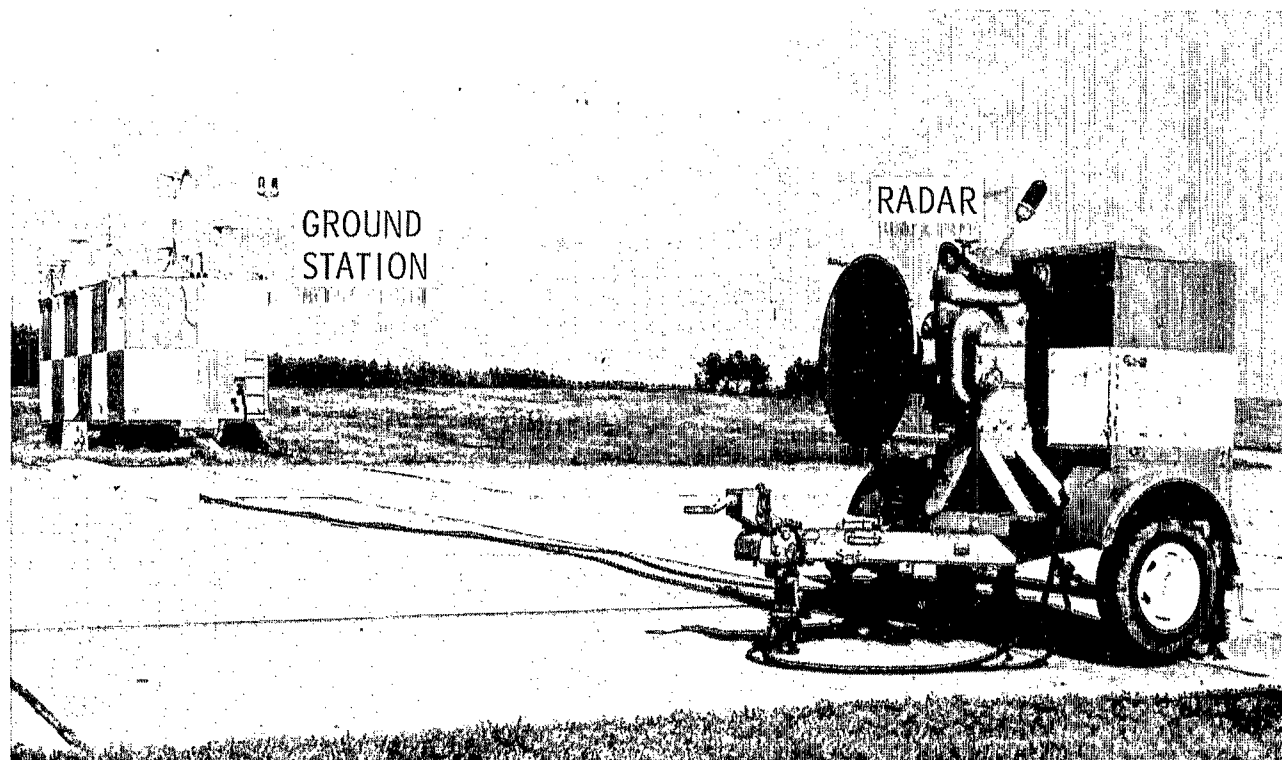
L-73-3043.1

Figure 2.- GSN-5 precision tracking radar.
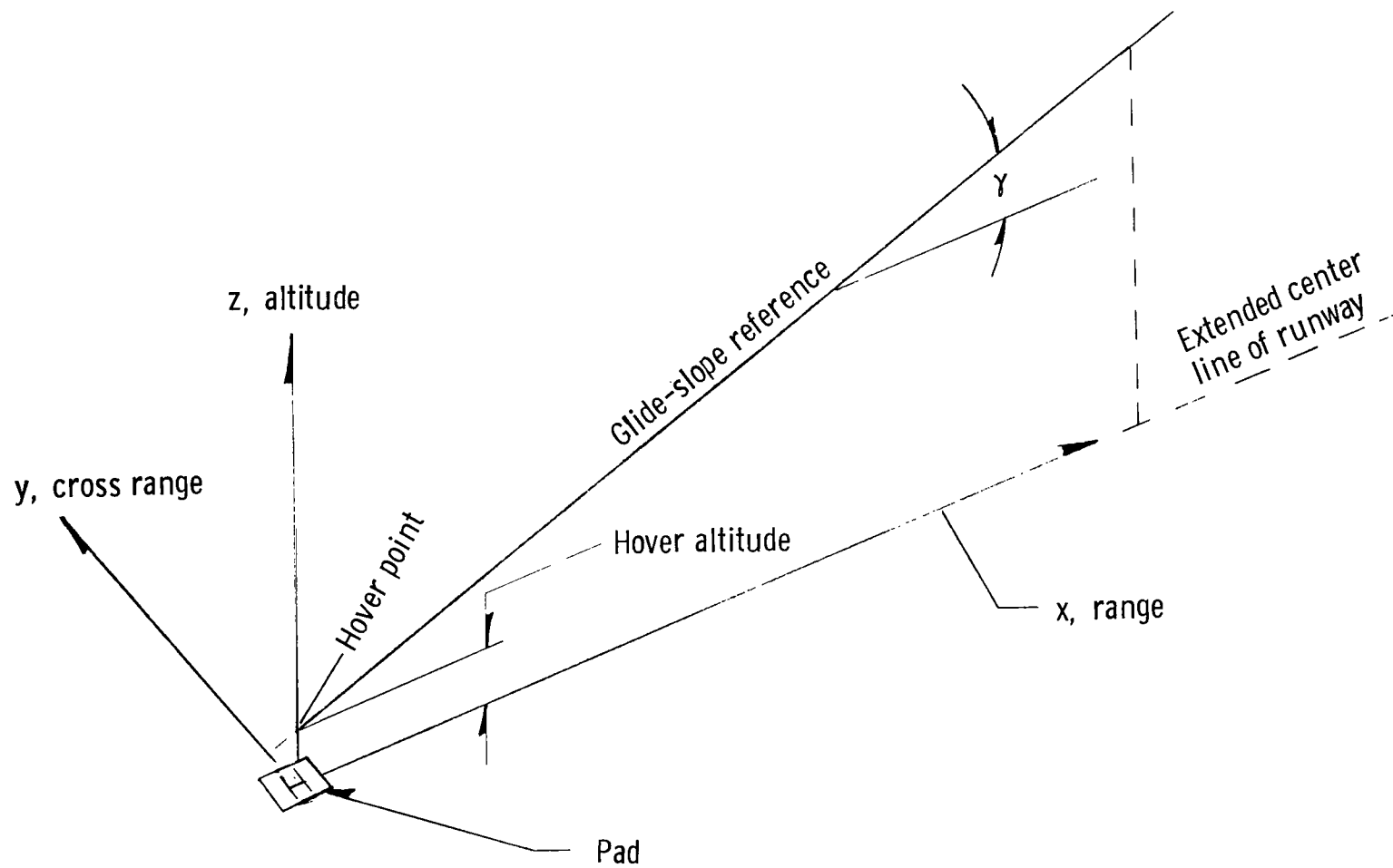
Figure 3.- Approach coordinate system.

	Altitude, m (ft)		
Airspeed, knots	150 (500)	300 (1000)	450 (1500)
50	4 | 12 / 30 / 5 | 9	4 | 5 / 24 / 4 | 11	1 | 12 / 26 / 4 | 9
80	2 | 12 / 28 / 4 | 10	2 | 10 / 29 / 5 | 12	2 | 11 / 28 / 4 | 11
100	3 | 6 / 22 / 4 | 9	5 | 5 / 25 / 4 | 11	2 | 6 / 24 / 4 | 12

A Number of approaches by helicopter 1
B Number of approaches by helicopter 2
C Number of approaches by helicopter 3
D Number of approaches by helicopter 4
E Total number of approaches by all helicopters

Figure 4.- Initial condition matrix.
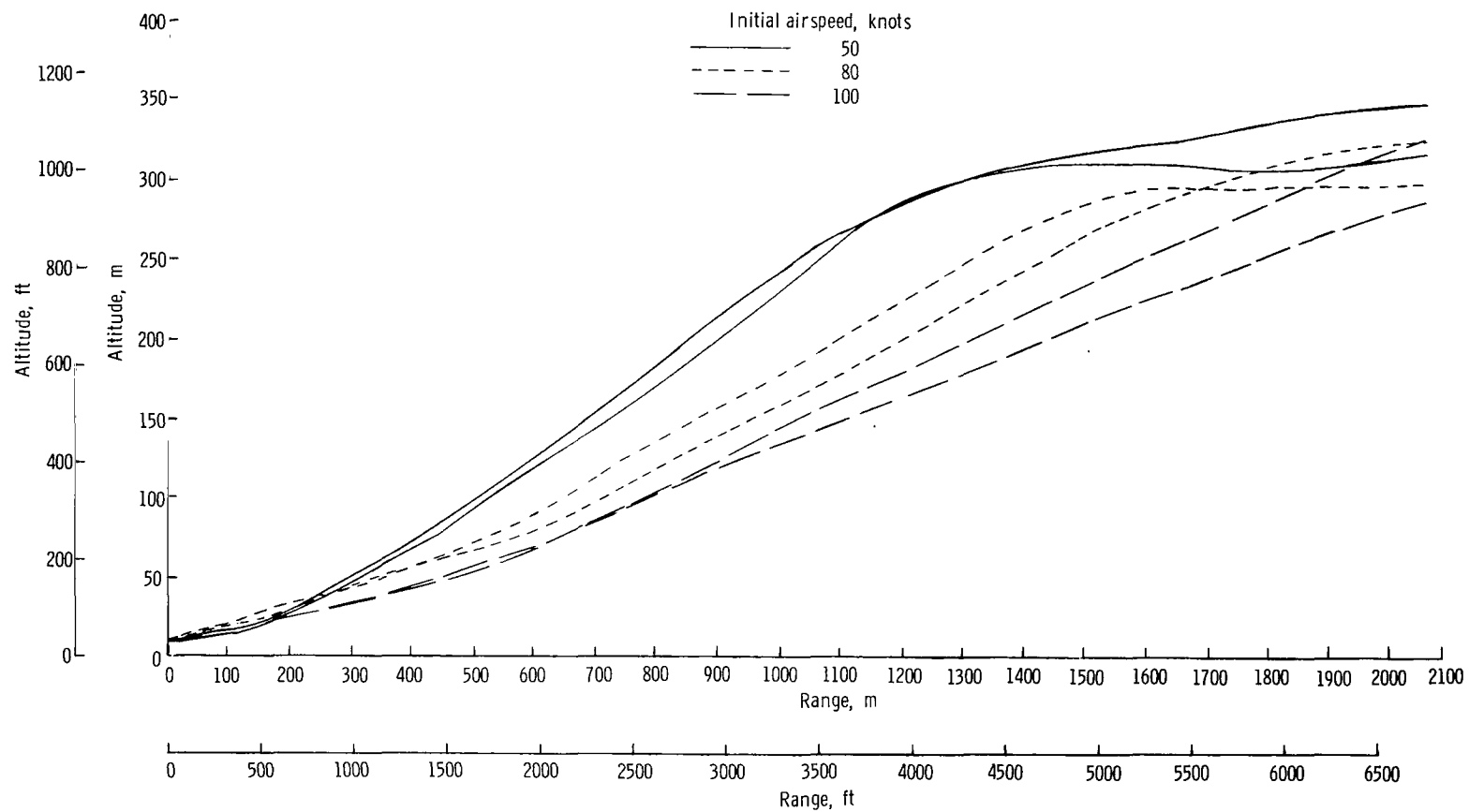
Figure 5.- Typical altitude profiles; initial altitude, 300 m (1000 ft).
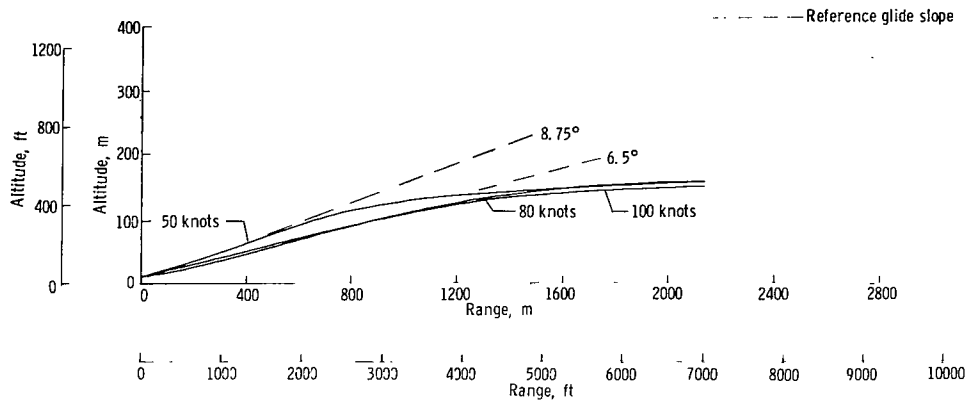
(a) Initial altitude, 150 m (500 ft).
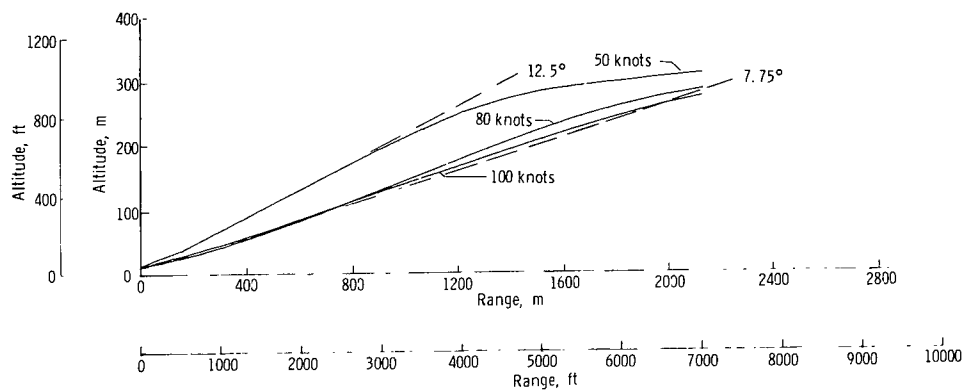
(b) Initial altitude, 300 m (1000 ft).
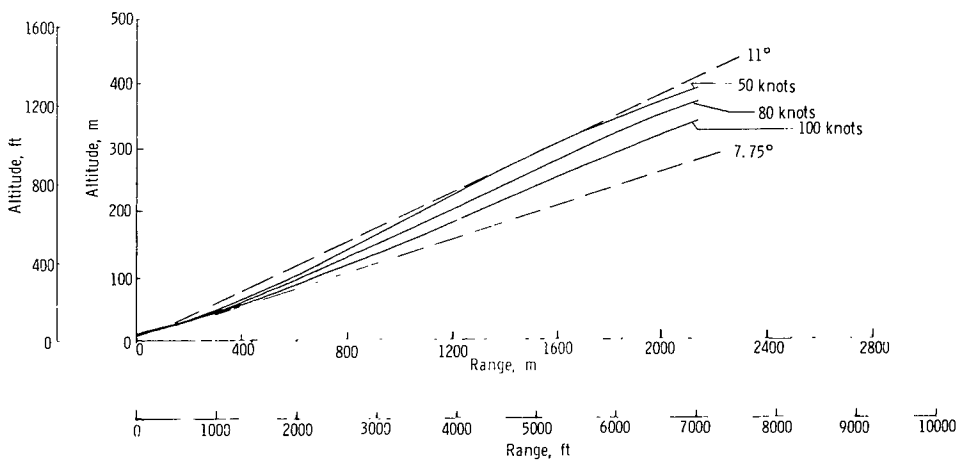
(c) Initial altitude, 450 m (1500 ft).

Figure 6.- Average VFR altitude profiles.
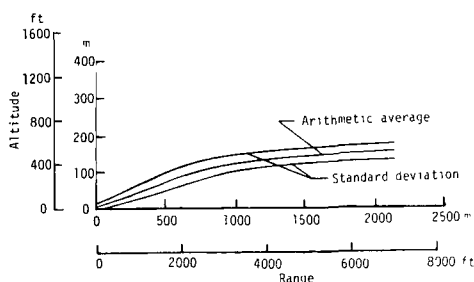
(a) 50 knots, 150 m (500 ft).   (b) 50 knots, 300 m (1000 ft).   (c) 50 knots, 450 m (1500 ft).
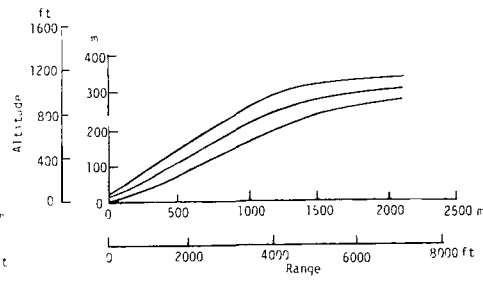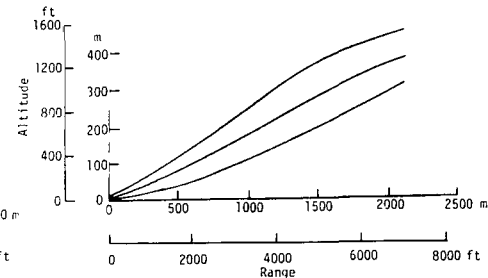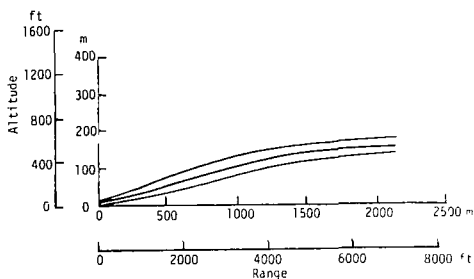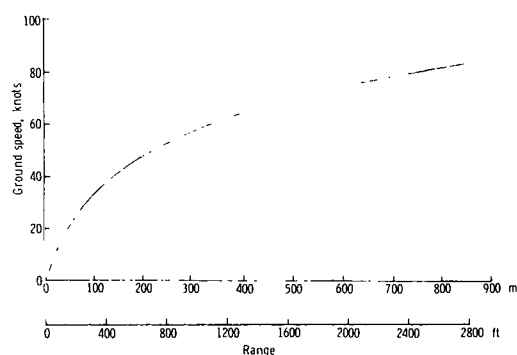
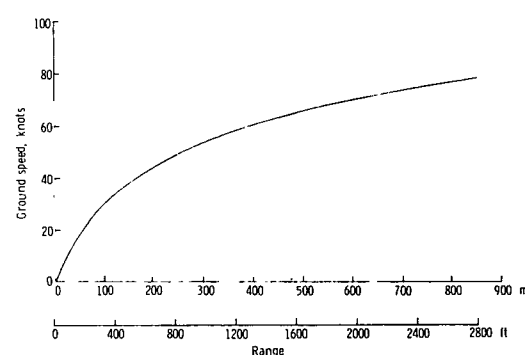(d) 80 knots, 150 m (500 ft).   (e) 80 knots, 300 m (1000 ft).   (f) 80 knots, 450 m (1500 ft).
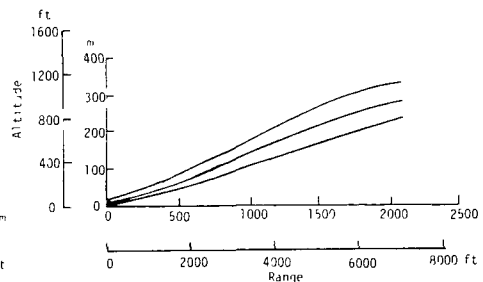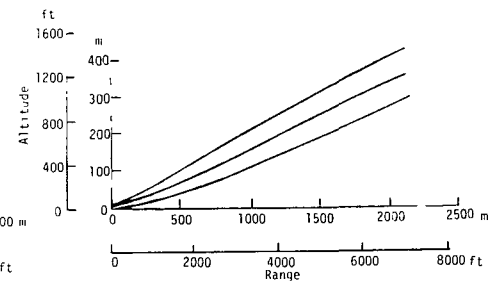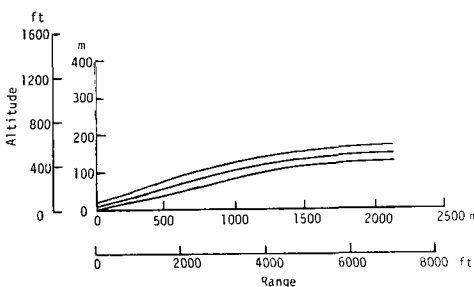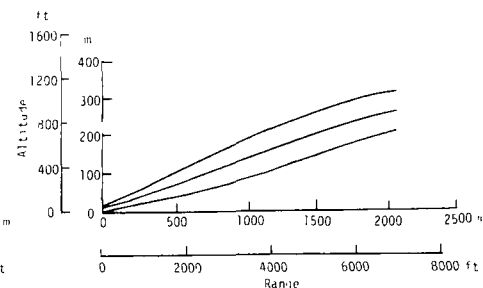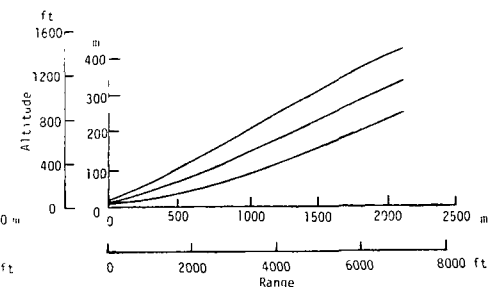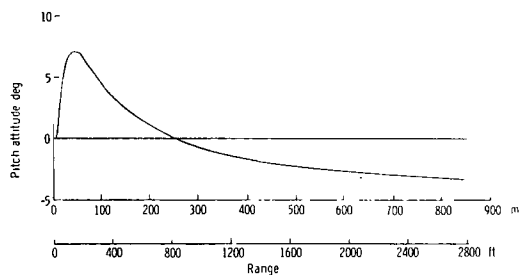
(g) 100 knots, 150 m (500 ft).   (h) 100 knots, 300 m (1000 ft).   (i) 100 knots, 450 m (1500 ft).

Figure 7.- Altitude standard-deviation envelopes for each initial airspeed and altitude. (Lines for arithmetic average and standard deviation as labeled on upper left are typical.)
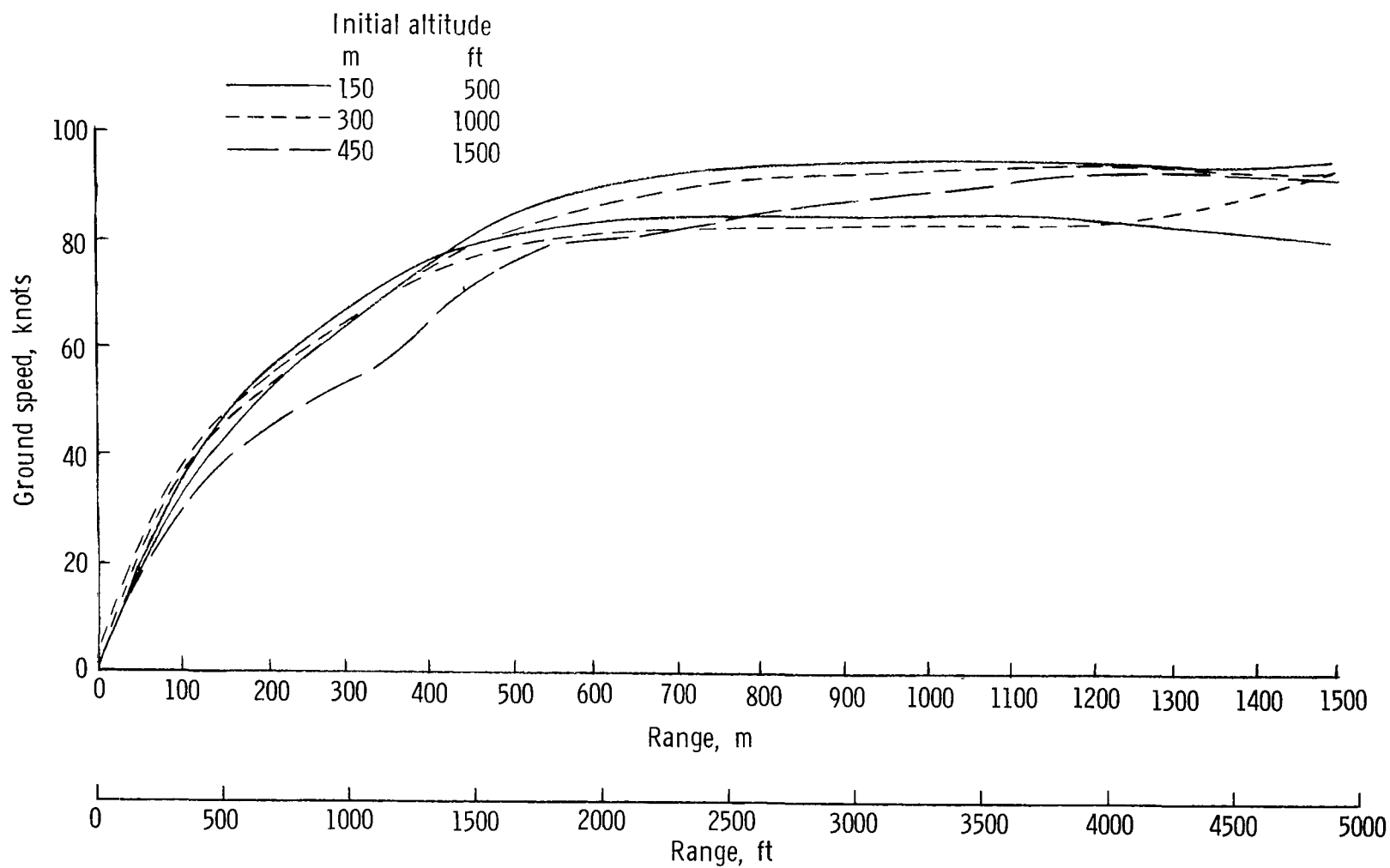
Figure 8.- Typical ground-speed profiles; initial airspeed, 80 knots.
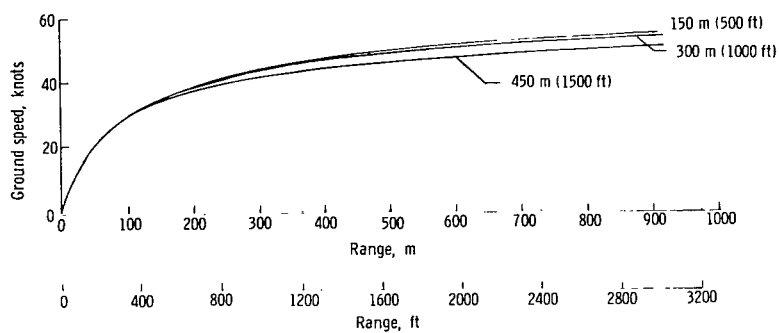
(a) Initial approach airspeed, 50 knots.
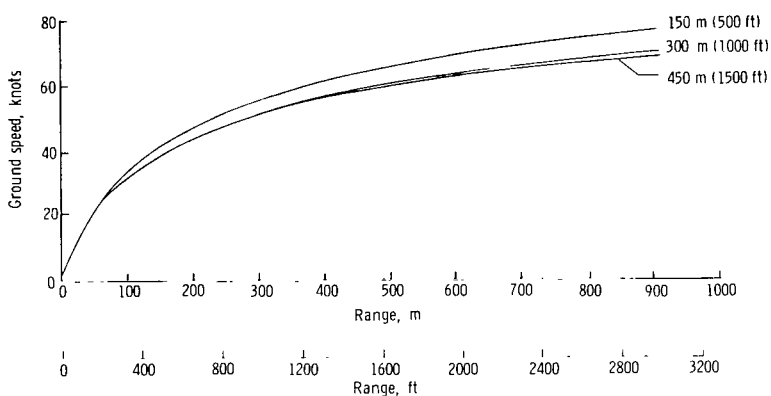
(b) Initial approach airspeed, 80 knots.
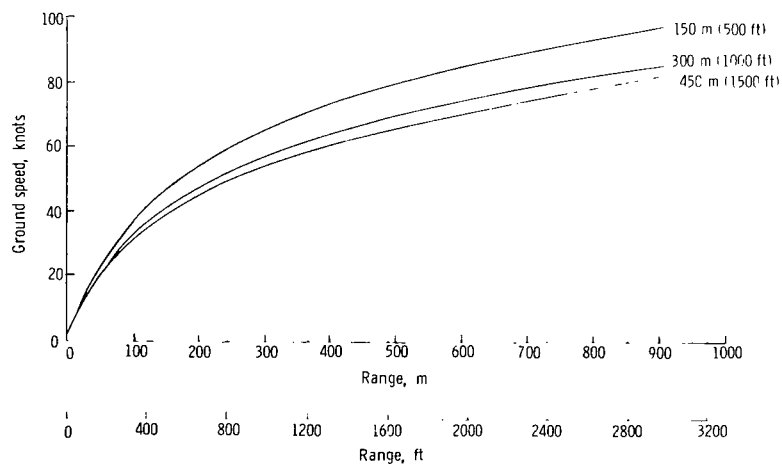
(c) Initial approach airspeed, 100 knots.

Figure 9.- Average ground-speed profiles.
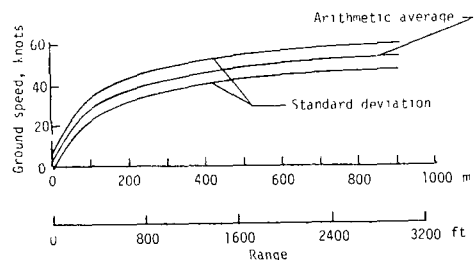
(a)   50 knots, 150 m (500 ft).
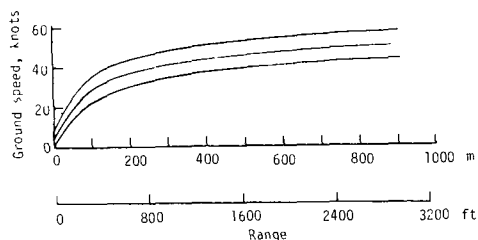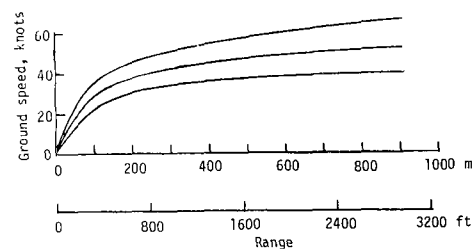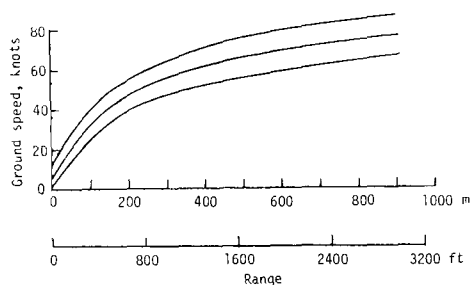
(b)   50 knots, 300 m (1000 ft).

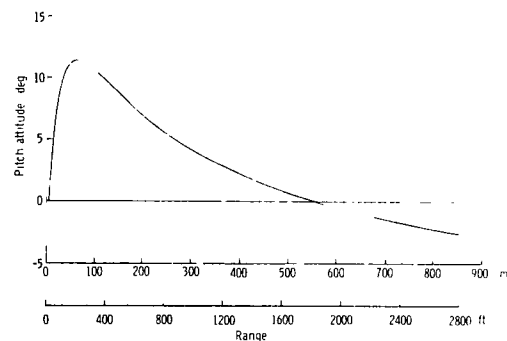(c)   50 knots, 450 m (1500 ft).
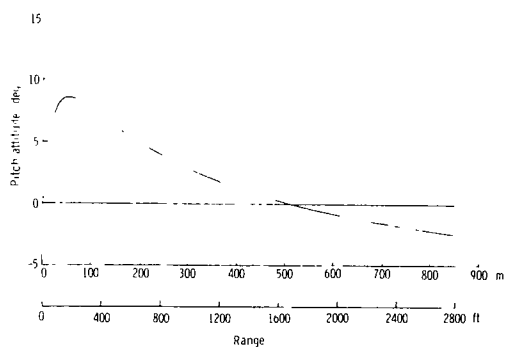
(d)   80 knots, 150 m (500 ft).
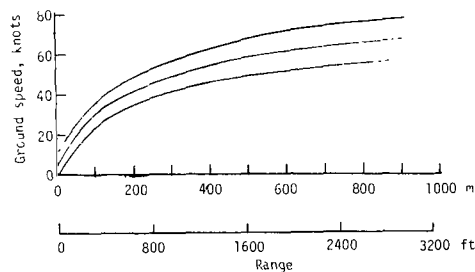
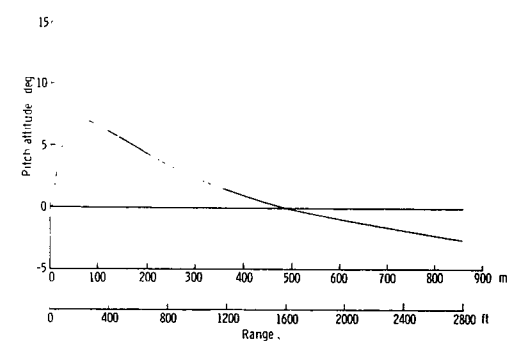(e)   80 knots, 300 m (1000 ft).
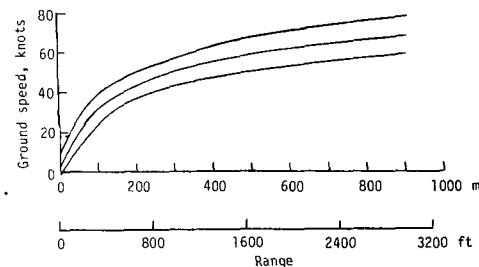
(f)   80 knots, 450 m (1500 ft).
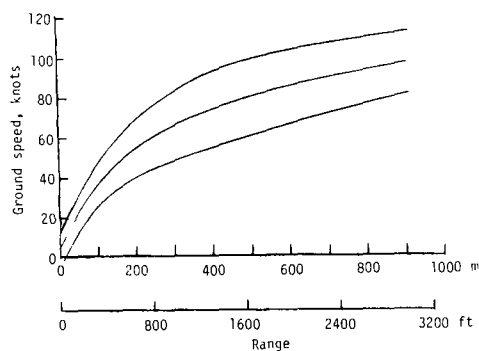
(g)   100 knots, 150 m (500 ft).
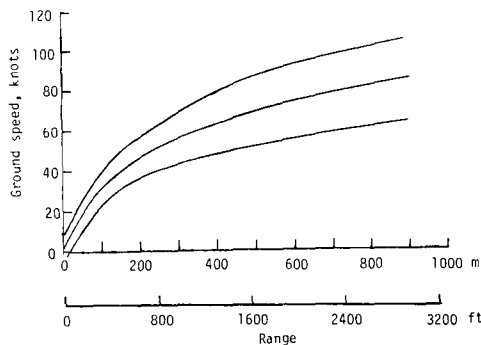
(h)   100 knots, 300 m (1000 ft).
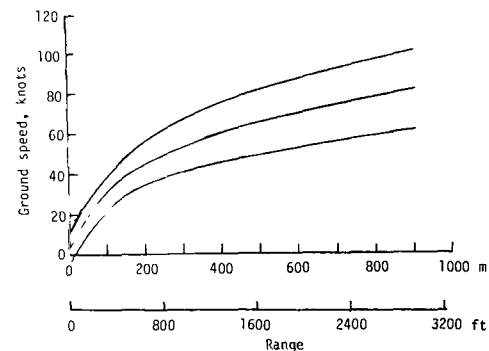
(i)   100 knots, 450 m (1500 ft).

Figure 10.- Ground-speed profiles for each initial airspeed and altitude. (Lines for arithmetic average and standard deviation as labeled on upper left are typical.)
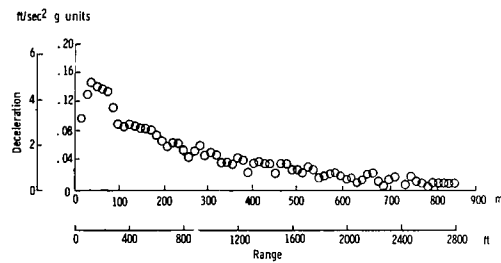
(a) 50 knots, 150 m (500 ft). (b) 50 knots, 300 m (1000 ft). (c) 50 knots, 450 m (1500 ft).
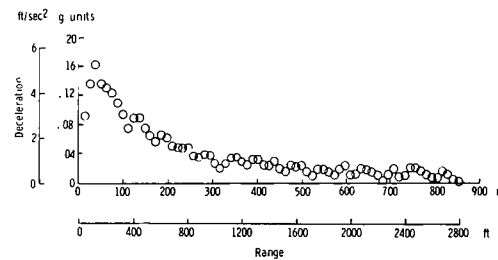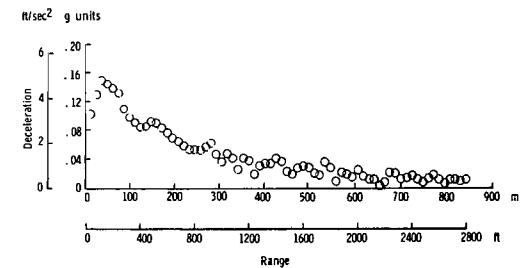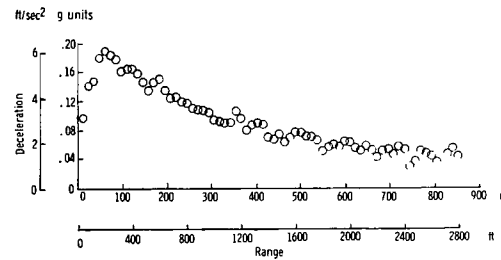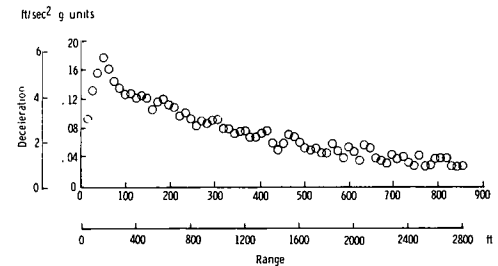
(d) 80 knots, 150 m (500 ft). (e) 80 knots, 300 m (1000 ft). (f) 80 knots, 450 m (1500 ft).
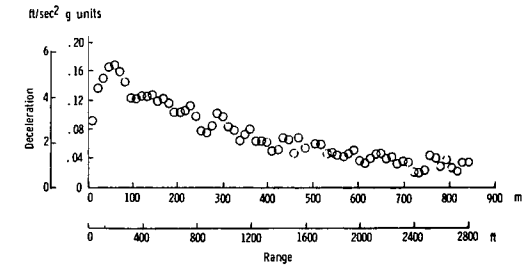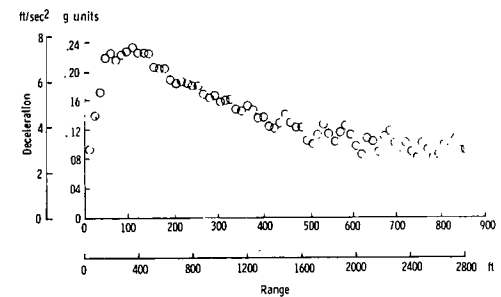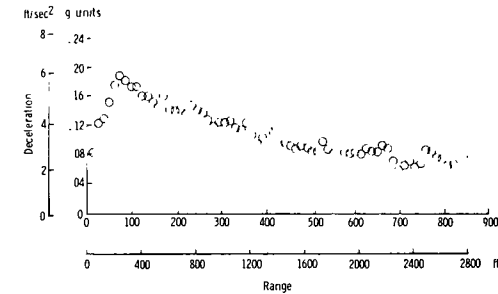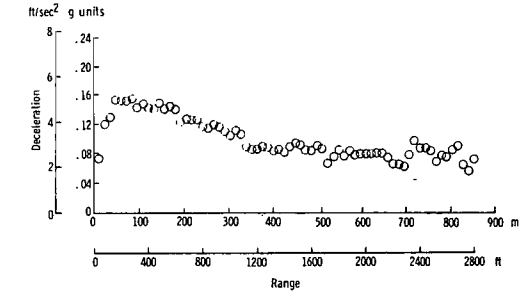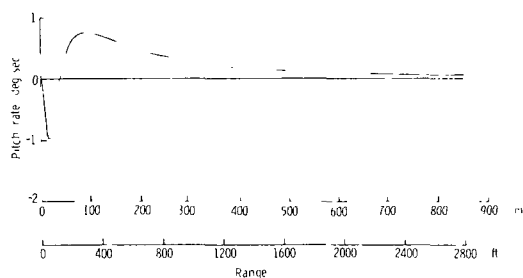
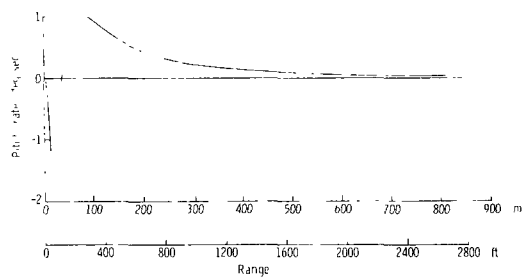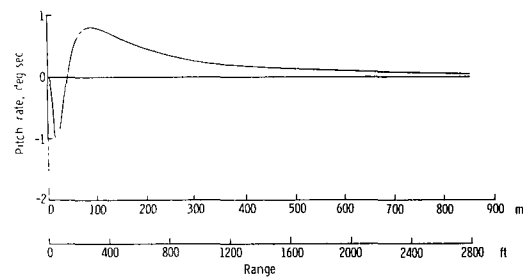(g) 100 knots, 150 m (500 ft). (h) 100 knots, 300 m (1000 ft). (i) 100 knots, 450 m (1500 ft).

Figure 11.- Visual deceleration profiles for different airspeed and altitude conditions.
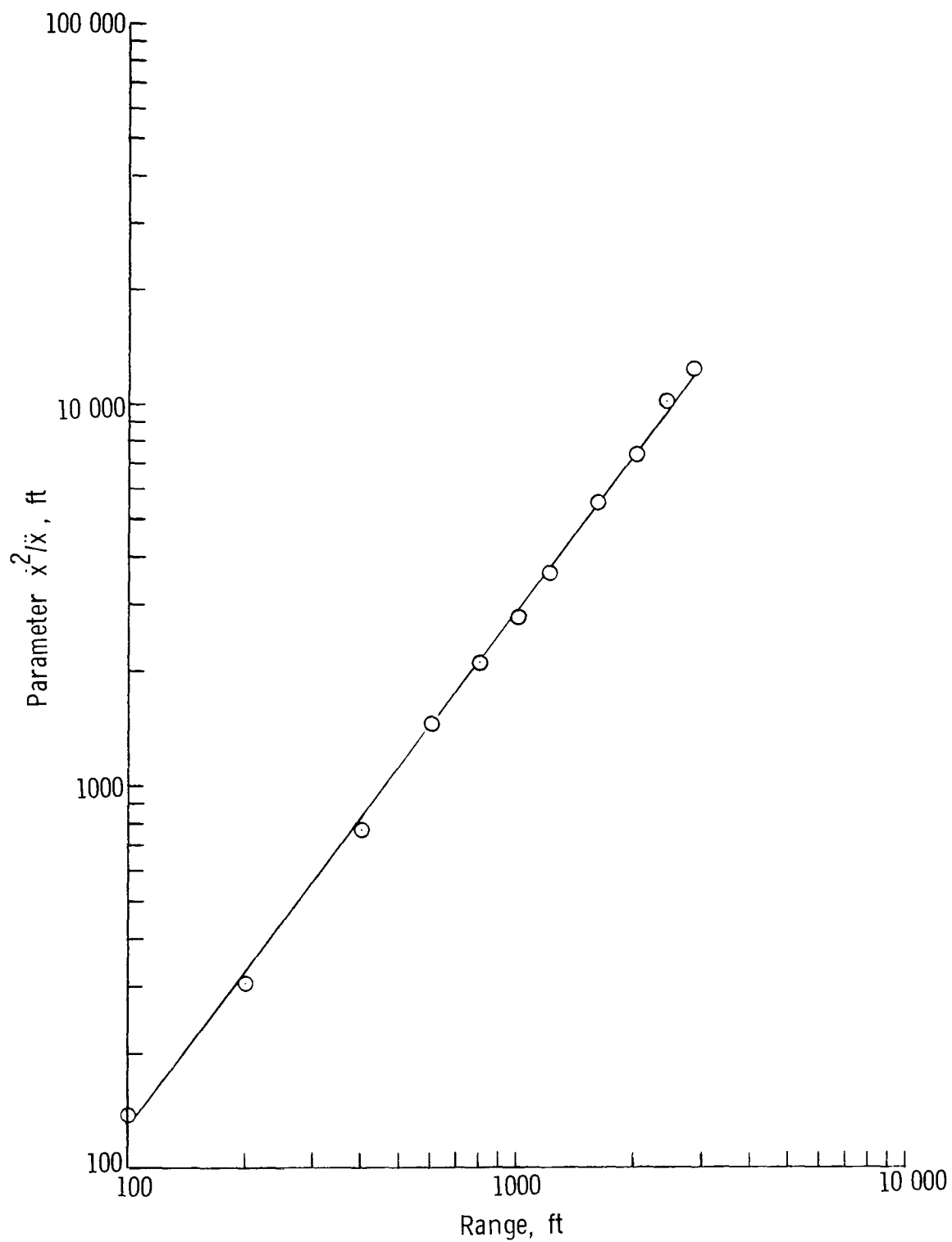
Figure 12.- Logarithmic plot of parameter $\dot{x}^2/\ddot{x}$ against range.
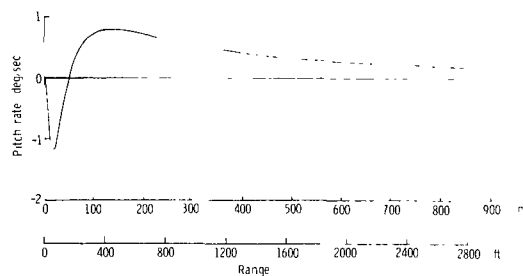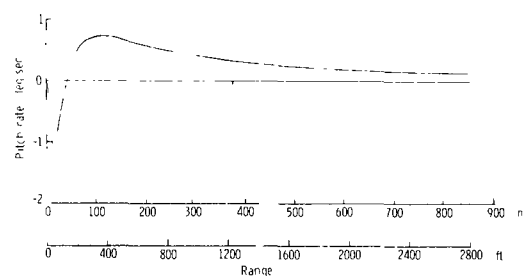(1 ft = 0.3048 m.)
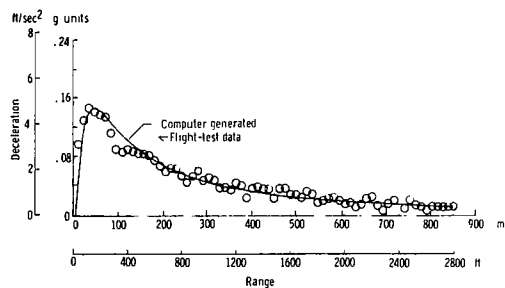
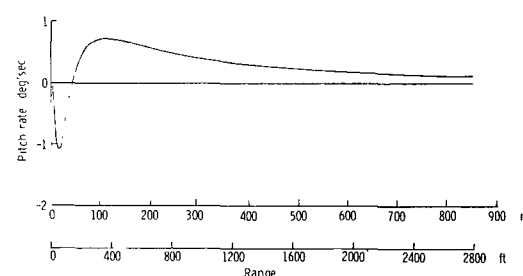(a) 50 knots, 150 m (500 ft).　　(b) 50 knots, 300 m (1000 ft).　　(c) 50 knots, 450 m (1500 ft).
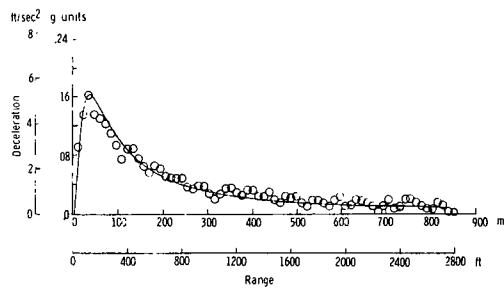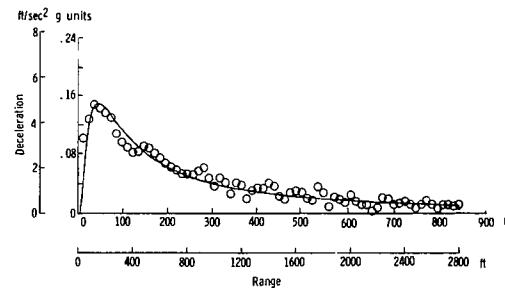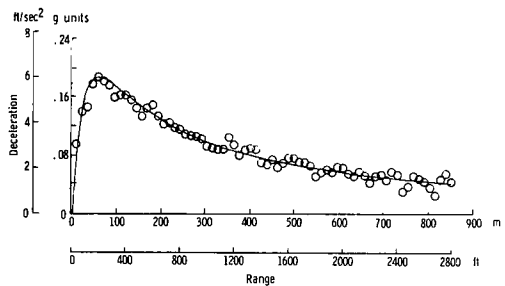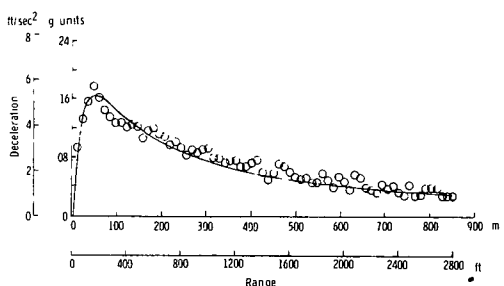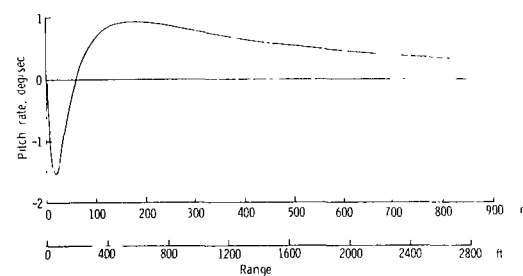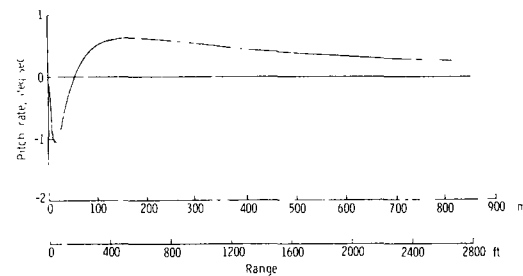
(d) 80 knots, 150 m (500 ft).　　(e) 80 knots, 300 m (1000 ft).　　(f) 80 knots, 450 m (1500 ft).
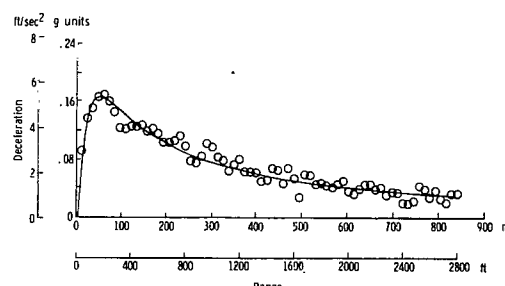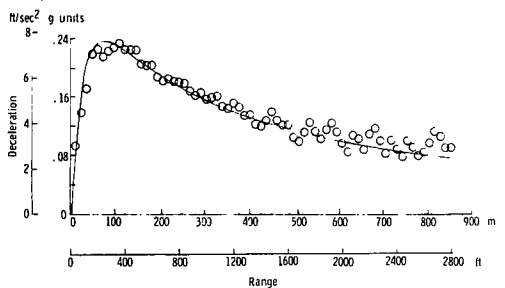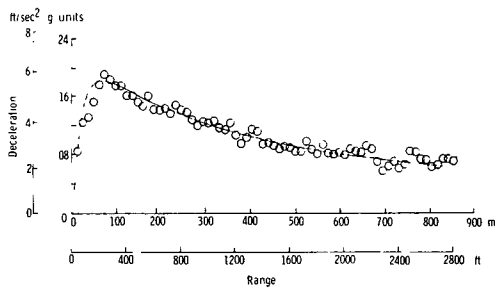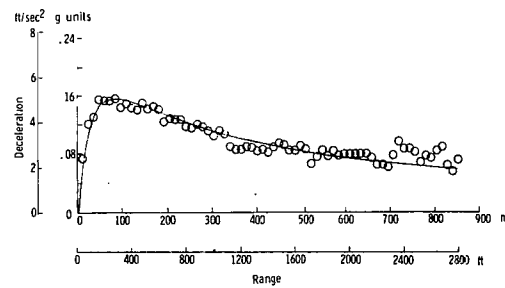
(g) 100 knots, 150 m (500 ft).　　(h) 100 knots, 300 m (1000 ft).　　(i) 100 knots, 450 m (1500 ft).

Figure 13.- Computer-generated deceleration profiles for different airspeed and altitude conditions.
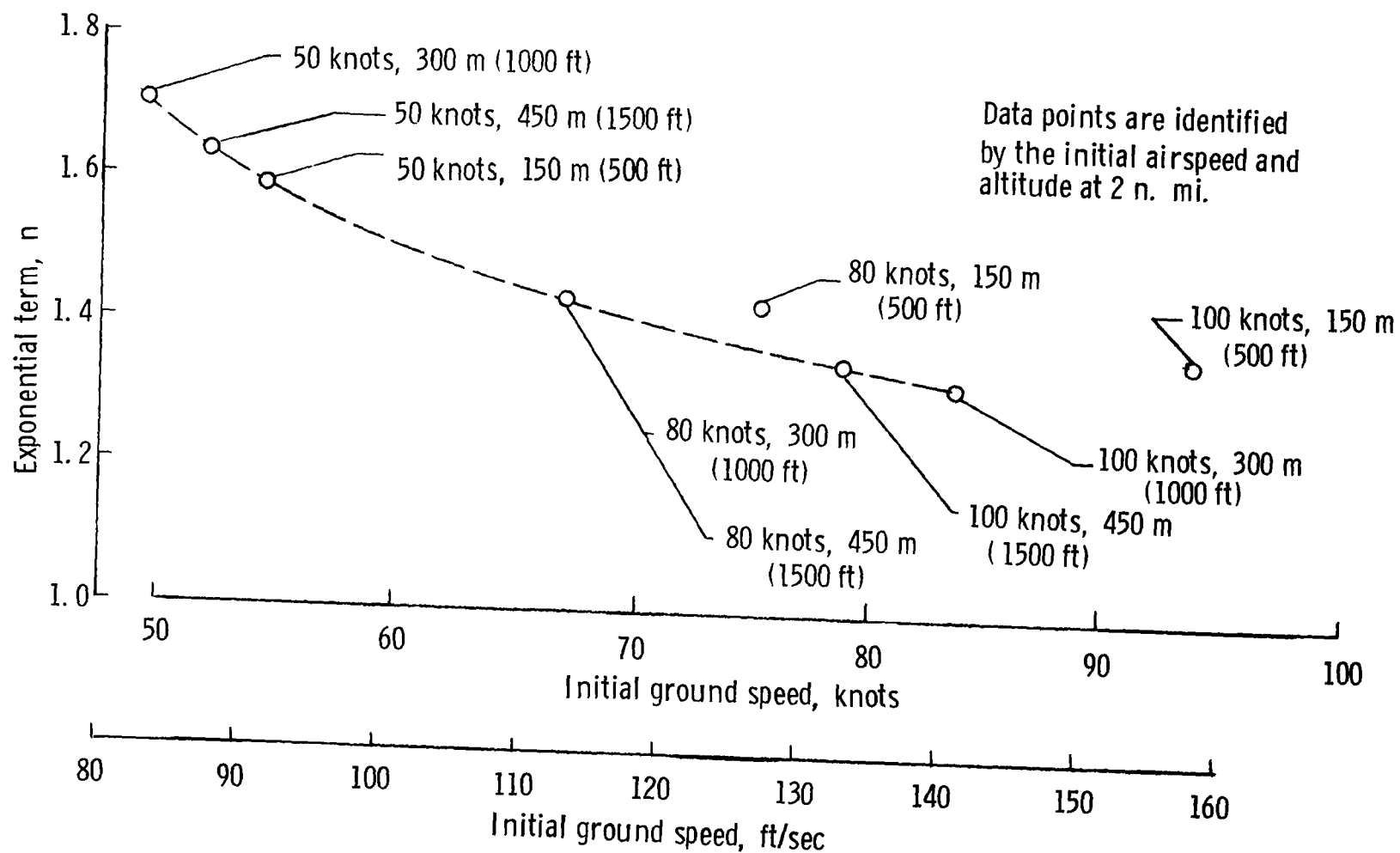
Figure 14.- Exponential term n plotted against initial ground speed at 850 m (2800 ft) range.
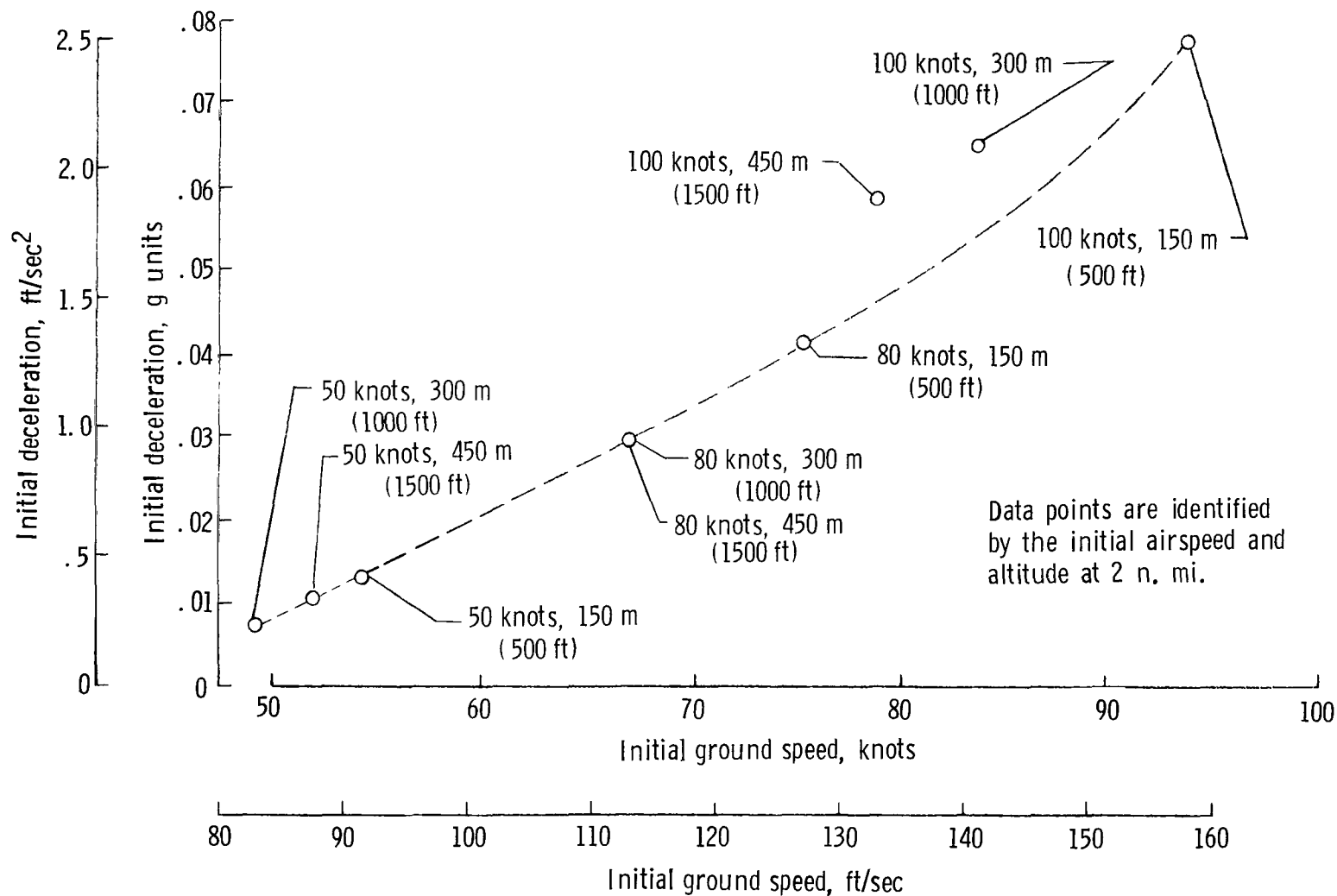
Figure 15.- Initial deceleration plotted against initial ground speed at 850 m (2800 ft) range.
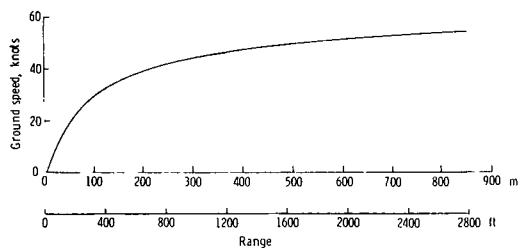
(a) 50 knots, 150 m (500 ft).
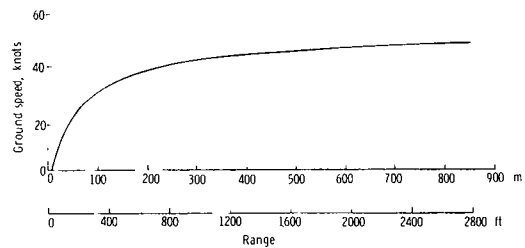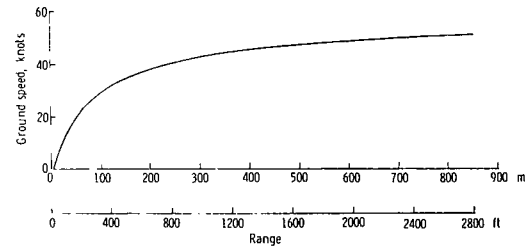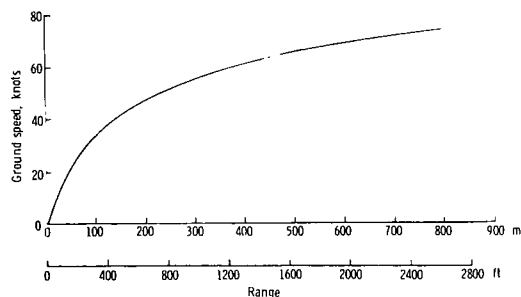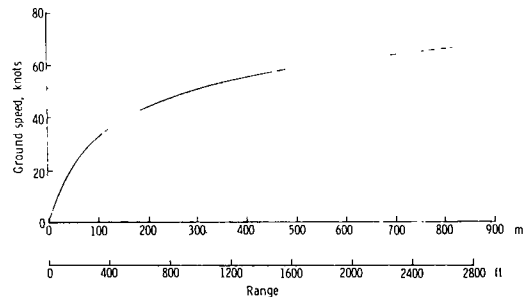
(b) 50 knots, 300 m (1000 ft).

(c) 50 knots, 450 m (1500 ft).

(d) 80 knots, 150 m (500 ft).

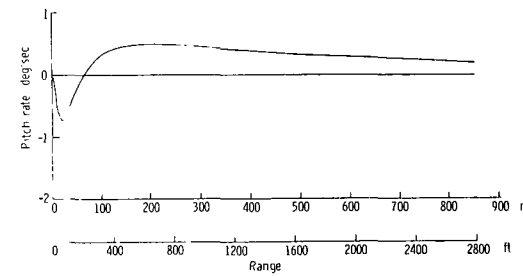(e) 80 knots, 300 m (1000 ft).
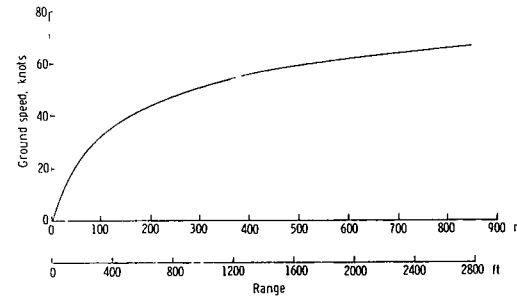
(f) 80 knots, 450 m (1500 ft).
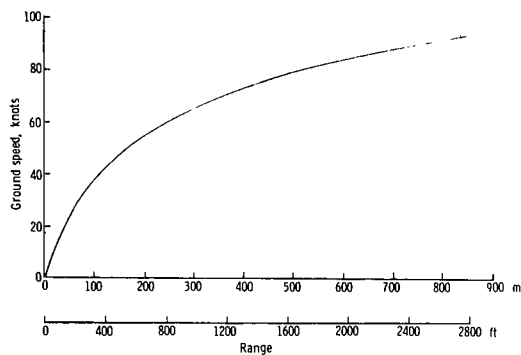
(g) 100 knots, 150 m (500 ft).

(h) 100 knots, 300 m (1000 ft).

(i) 100 knots, 450 m (1500 ft).

Figure 16.- Computer-generated ground-speed profiles for different airspeed and altitude conditions.
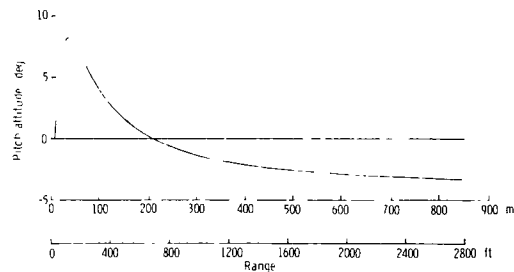
(a) 50 knots, 150 m (500 ft).

(b) 50 knots, 300 m (1000 ft).
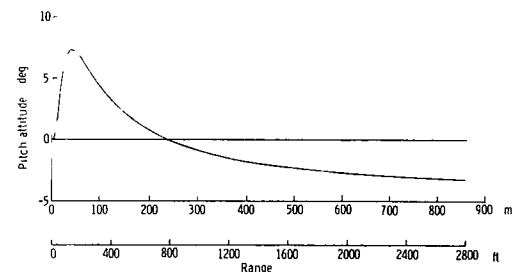
(c) 50 knots, 450 m (1500 ft).
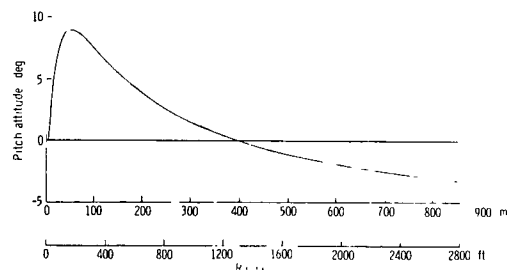
(d) 80 knots, 150 m (500 ft).
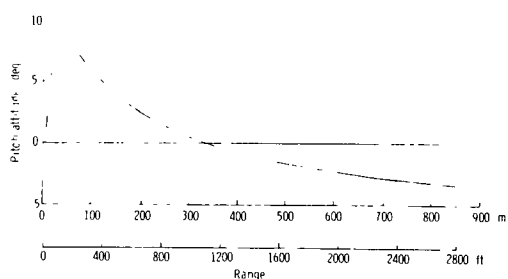
(e) 80 knots, 300 m (1000 ft).
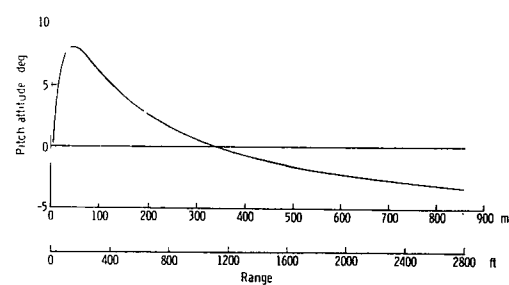
(f) 80 knots, 450 m (1500 ft).
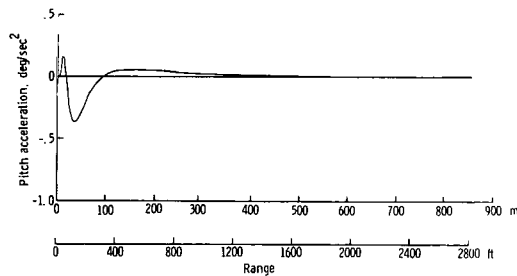
(g) 100 knots, 150 m (500 ft).
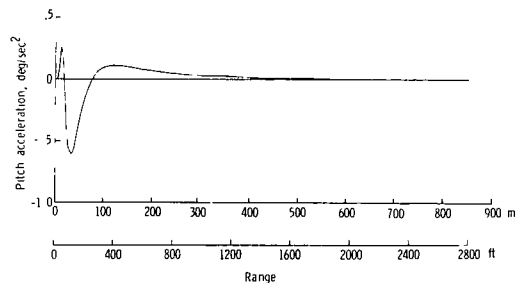
(h) 100 knots, 300 m (1000 ft).
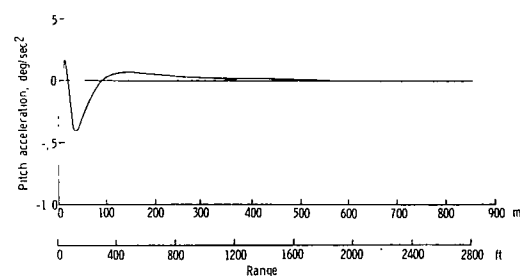
(i) 100 knots, 450 m (1500 ft).

Figure 17.- Nominal pitch-attitude profiles for different airspeed and altitude conditions.
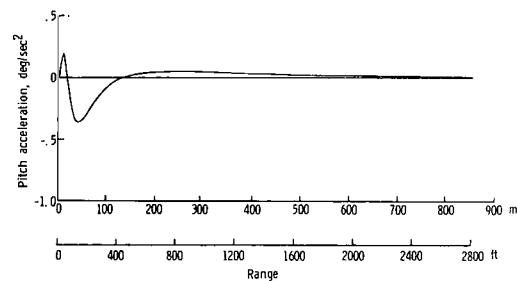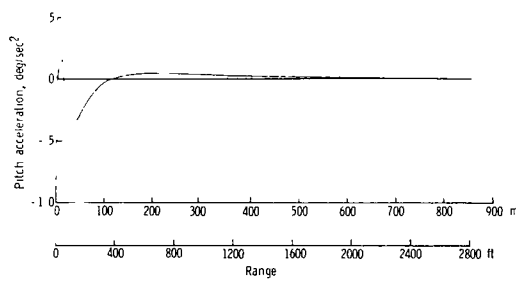
(a)   50 knots, 150 m (500 ft).
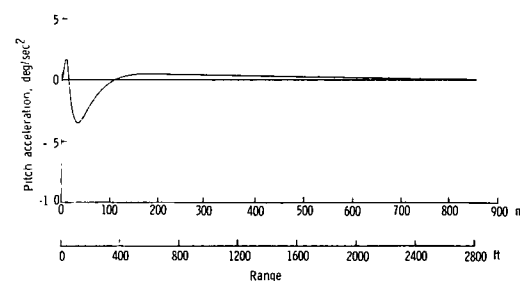
(b)   50 knots, 300 m (1000 ft).

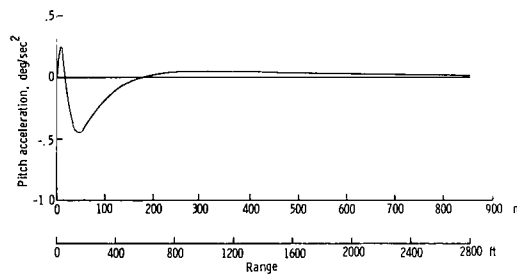(c)   50 knots, 450 m (1500 ft).

(d)   80 knots, 150 m (500 ft).

(e)   80 knots, 300 m (1000 ft).

(f)   80 knots, 450 m (1500 ft).

(g)   100 knots, 150 m (500 ft).

(h)   100 knots, 300 m (1000 ft).

(i)   100 knots, 450 m (1500 ft).

Figure 18.- Nominal pitch-rate profiles for different airspeed and altitude conditions.

(a) 50 knots, 150 m (500 ft).

(b) 50 knots, 300 m (1000 ft).

(c) 50 knots, 450 m (1500 ft).

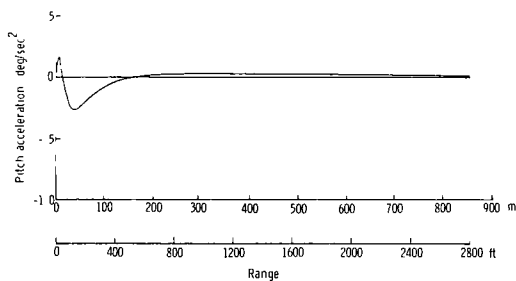(d) 80 knots, 150 m (500 ft).

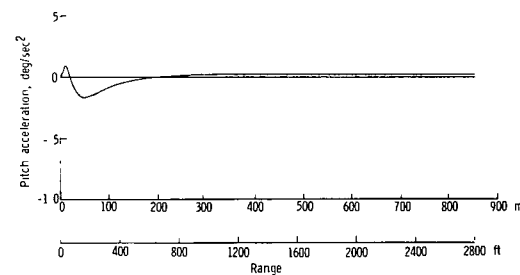(e) 80 knots, 300 m (1000 ft).

(f) 80 knots, 450 m (1500 ft).

(g) 100 knots, 150 m (500 ft).

(h) 100 knots, 300 m (1000 ft).

(i) 100 knots, 450 m (1500 ft).

Figure 19.- Nominal pitch-acceleraion profiles for different airspeed and altitude conditions.

	Initial altitude, m (ft)					
	150 (500)		**300 (1000)**		**450 (1500)**	

Initial airspeed, knots

	A	B	A	B	A	B
50	73	7.2	94	8.27	86	7.32
E		0.148		0.165		0.149
	-1.0	-0.367	-1.35	-0.620	-1.03	-0.41
80	49	9.01	49	8.06	49	8.06
E		0.187		0.167		0.167
	-1.18	-0.37	-1.11	-0.35	-1.11	-0.35
100	41	11.5	42	8.63	51	7.14
E		0.239		0.181		0.157
	-1.53	-0.45	-1.05	-0.27	-0.737	-0.17

A	B
	E	
C	D
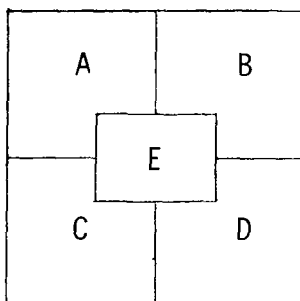
A   Deceleration time interval, sec
B   Maximum pitch attitude, deg
C   Maximum pitch rate, deg/sec
D   Maximum pitch acceleration, deg/sec^2
E   Maximum deceleration, g units

Figure 20.- Summary of maximum profile parameter values for visual approaches.
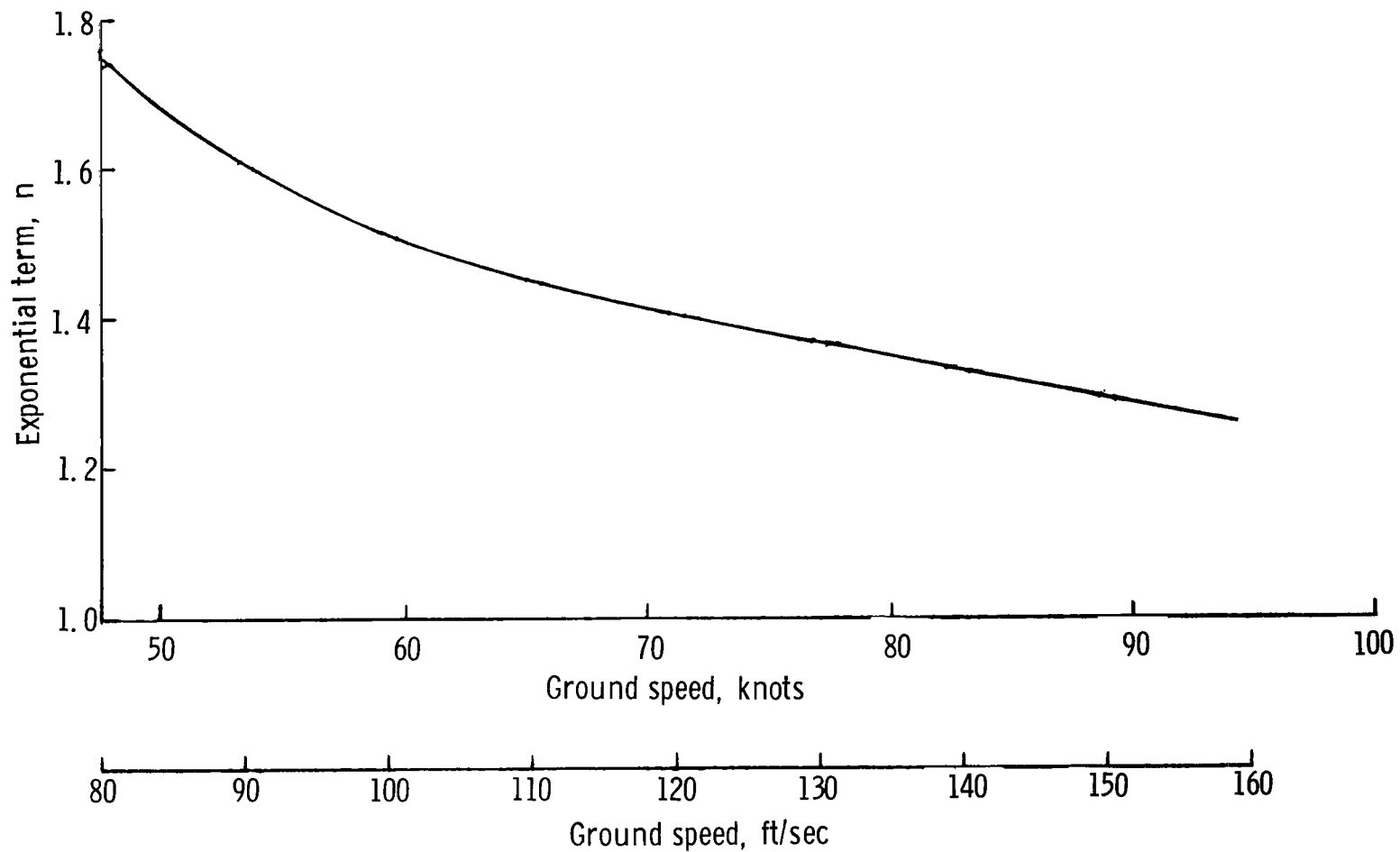
Figure 21.- Exponential term n as a function of ground speed at 850 m (2800 ft) range.
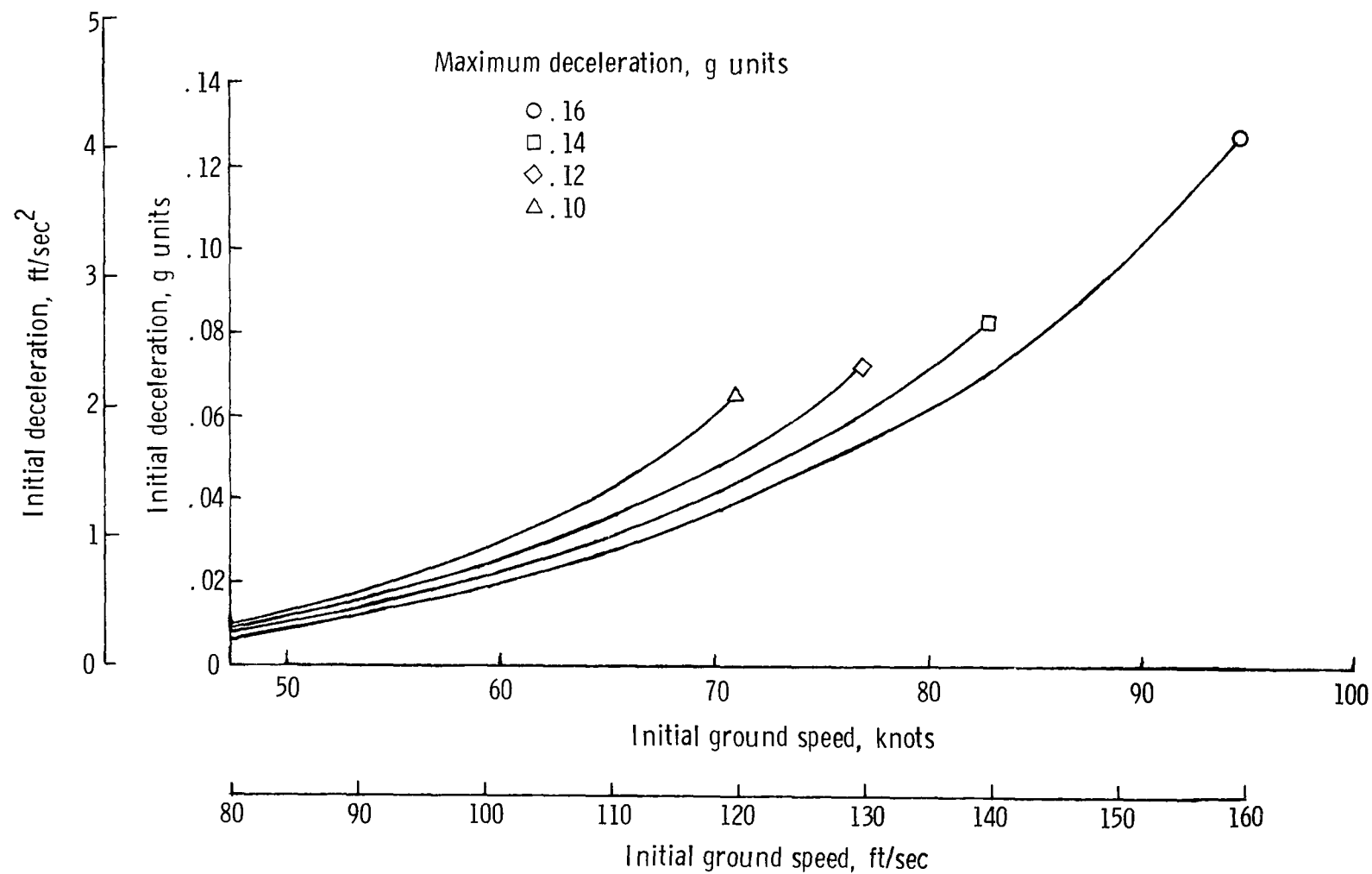
Figure 22.- Initial deceleration as a function of initial ground speed at 850 m (2800 ft) range.

Figure 23.- Summary of results from computer-generated profiles.

933 001 C1 U, A 761119 S00903DS
DEPT OF THE AIR FORCE
AF WEAPONS LABORATORY
ATTN: TECHNICAL LIBRARY (SUL)
KIRTLAND AFB NM 87117

"The aeronautical and space activities of the United States shall be conducted so as to contribute . . . to the expansion of human knowledge of phenomena in the atmosphere and space. The Administration shall provide for the widest practicable and appropriate dissemination of information concerning its activities and the results thereof."
—NATIONAL AERONAUTICS AND SPACE ACT OF 1958

NASA SCIENTIFIC AND TECHNICAL PUBLICATIONS

TECHNICAL REPORTS: Scientific and technical information considered important, complete, and a lasting contribution to existing knowledge.

TECHNICAL NOTES: Information less broad in scope but nevertheless of importance as a contribution to existing knowledge.

TECHNICAL MEMORANDUMS: Information receiving limited distribution because of preliminary data, security classification, or other reasons. Also includes conference proceedings with either limited or unlimited distribution.

CONTRACTOR REPORTS: Scientific and technical information generated under a NASA contract or grant and considered an important contribution to existing knowledge.

TECHNICAL TRANSLATIONS: Information published in a foreign language considered to merit NASA distribution in English.

SPECIAL PUBLICATIONS: Information derived from or of value to NASA activities. Publications include final reports of major projects, monographs, data compilations, handbooks, sourcebooks, and special bibliographies.

TECHNOLOGY UTILIZATION PUBLICATIONS: Information on technology used by NASA that may be of particular interest in commercial and other non-aerospace applications. Publications include Tech Briefs, Technology Utilization Reports and Technology Surveys.

Details on the availability of these publications may be obtained from:

SCIENTIFIC AND TECHNICAL INFORMATION OFFICE

NATIONAL AERONAUTICS AND SPACE ADMINISTRATION

Washington, D.C. 20546